Transport through driven nanoscale conductors

Habilitationsschrift

für das Fach Theoretische Physik
an der Mathematisch-Naturwissenschaftlichen Fakultät
der Universität Augsburg

vorgelegt von
Dr. Sigmund Kohler

Augsburg, im Juni 2004

Abstract

We consider the electron transport through driven tight-binding systems. For the theoretical description, a Floquet scattering approach and a Floquet master equation approach are derived. Both formalisms are particularly suited for the exact treatment of non-adiabatic driving. While the scattering approach describes coherent transport exactly, the master equation approach is suitable for a rather direct extension to the case of electron-phonon interaction. Moreover, we derive an expression for the corresponding transport noise which in the driven case depends on the phases of the transmission amplitudes. With these formalisms, we study different situations like the transport through driven molecular wires, the dynamics of coherent quantum ratchets, and the control of current and noise by ac fields.

Contents

1 Introduction **1**
1.1 Experimental motivation 3
1.2 Wire-lead model 4
1.3 Transport theory 7

2 Floquet transport theory **11**
2.1 Floquet master equation approach 11
2.2 Floquet scattering approach 14
2.3 High-frequency approximation 17

3 Transport through resonantly driven molecular wires **19**

4 Non-adiabatic electron pumping **23**

5 Coherent current control **29**

6 Summary and outlook **33**

Acknowledgements **35**

References **37**

Selected publications **43**

1 Introduction

During the last years, the present author has contributed to the theoretical investigation of three types of time-dependent open quantum systems, namely split atomic Bose-Einstein condensates in time-dependent traps, driven qubits coupled to a heat bath, and nanoscale conductors under the influence of electromagnetic fields. A clear focus has been put on the latter type of systems, in particular on molecular wires in laser fields and on coupled quantum dots under the influence of microwave radiation. The aim of this survey is to review the corresponding publications which are presented in the appendix.

Recently, considerable progress has been achieved in contacting single molecules by nanoelectrodes. This allows to apply a transport voltage and to measure the resulting electrical current [1–6]. For the corresponding theoretical investigations, two lines of research are presently followed. The one is the *ab-initio* computation of the orbitals relevant for the motion of excess charges through the molecular wire [7, 8]. The other line employs rather universal models to gain a qualitative understanding of the transport mechanisms involved [9–14]. Two particular problems addressed within model calculations are the conduction mechanism in the presence of electron-phonon coupling [10] and the length dependence of the current-voltage characteristics [9, 13]. The present work also employs rather universal models: We describe the molecules by a linear arrangement of tight-binding levels with the terminating sites attached to leads. This model also captures the physics of the so-called artificial molecules, i.e. coupled quantum dots and quantum dot arrays [15, 16].

One particular question in this context is the influence of excitations by electromagnetic fields and gates voltages on the electron transport. Such excitations bear intriguing phenomena like photon-assisted tunneling [16–19] and the adiabatic [20–22] and non-adiabatic pumping [23, 24] of electrons. From a fundamental point of view, these effects are of interest because the external fields enable selective electron excitations and allow to study their interplay with the underlying transport mechanism. In practical applications, time-dependent effects can be used to control and steer currents in coherent conductors. However, such control schemes can be valuable only if they operate at tolerable noise levels. Thus, the corresponding current noise is also of interest.

An intuitive description of the coherent electron transport through time-independent mesoscopic systems is provided by the Landauer scattering formula [25] and its various generalizations. Both the average current [26–29] and the transport noise characteristics [30] can be expressed in terms of the quantum transmission coefficients for the respective scattering channels. By contrast, the theory for driven quantum transport is less developed. Scattering of a single particle by arbitrary time-dependent potentials has been considered [31–33] without relating the resulting transmissions to a current between electron reservoirs. Such a relation is indeed non-trivial since the driving opens inelastic transport channels and, therefore, in contrast to the static case, an *ad hoc* inclusion of the Pauli principle is no longer unique. This gave rise to a discussion about "Pauli blocking factors" [34, 35]. In order to avoid such conflicts, one should start out from a many-particle

description. In this spirit, within a Green function approach, a formal solution for the current through a time-dependent conductor has been presented [36, 37] without taking advantage of the full Floquet theory for the wire and without obtaining a "scattering form" for the current in the driven case. The spectral density of the current fluctuations has been derived for the low-frequency ac conductance [38, 39] and the scattering by a slowly time-dependent potential [40]. For arbitrary driving frequencies, the noise can be characterized by its zero-frequency component. A remarkable feature of the current noise in the presence of time-dependent fields is its dependence on the phase of the transmission *amplitudes* [A5, A9, 40]. By clear contrast, both the noise in the static case [30] and the current in the driven case depend solely on transmission *probabilities*.

In Chap. 2, we derive within a Floquet approach explicit expressions for both the current and the noise properties of the electron transport through a driven nanoscale conductor under the influence of time-dependent forces [A5, A9]. This approach is applicable to arbitrary periodically driven tight-binding systems and, in particular, is valid for arbitrary driving strength and extends beyond the adiabatic regime. The dynamics of the electrons is solved by integrating the Heisenberg equations of motion for the electron creation and annihilation operators in terms of the single-particle propagator. For this propagator, in turn, we provide a solution within a generalized Floquet approach. Such a treatment is valid only for effectively non-interacting electrons, i.e., when no strong correlations occur. Moreover, this Floquet scattering approach cannot be generalized straightforwardly to the case with additional electron-vibrational coupling. Better suited for this situation is a quantum kinetic equation formalism which, however, is perturbative in both the wire-lead coupling and the electron-vibrational coupling [A4, A10].

An experimental starting point for the investigation of the influence of electromagnetic fields on molecular conduction is the excitation of electrons to higher orbitals of the contacted molecule. In molecular physics, specific excitations are usually performed with laser fields. The resulting changes of the current through a contacted molecule due to the influence of a laser field are studied in Chap. 3. In particular, we focus on the modification of the length dependence of the conductivity [A2, A8].

An intriguing phenomenon in strongly driven systems is the so-termed ratchet effect [41–44], originally discovered for overdamped classical Brownian motion in asymmetric nonequilibrium systems. Counter-intuitively to the second law of thermodynamics, one then observes a directed transport although none of the acting forces possesses a net bias. This effect has been established also within the regime of dissipative, incoherent quantum Brownian motion [45, 46]. A mesoscopic device related to ratchets is an electron pump [20–24, 47, 48] which indeed might be regarded as a localized ratchet. In Chap. 4, we study the possibilities for molecular wires to act as coherent quantum ratchets and also explore the crossover from pumps to ratchets. Thereby, we investigate ratchets in the coherent quantum regime where they have not been studied previously [A1, A4, A10].

The tunneling dynamics of a particle in a bistable potential can be altered significantly by ac fields. In particular, it is possible to bring tunneling to a standstill by the purely coherent influence of a time-periodic driving [49]. This so-called coherent destruction of tunneling has also been found in other systems [50–52]. In Chap. 5, we address the question whether a related effect exists also for the electron transport through a driven

conductor between two leads. Moreover, we study the noise properties of the resulting transport process [A3, A5, A6, A9, A10].

Before going *in medias res*, however, we discuss in this chapter the experimental background and introduce our working model. Moreover, we review some relevant theoretical approaches, namely Tien-Gordon theory, the scattering approach for static conductors, and a master equation approach.

1.1 Experimental motivation

Coupled quantum dots

The experimental achievement of the coherent coupling of quantum dots [15] enabled the measurement of intriguing phenomena in mesoscopic transport [16]. A remarkable feature of coupled quantum dots—the so-called artificial molecules with the single dots representing the atoms—is that the energy levels of each "atom" can be controlled by an appropriate gate voltage. In particular, the highest occupied levels of neighboring dots can be tuned into resonance. At such resonances, the conductance as a function of the gate voltage exhibits a peak. This behavior is modified by the influence of microwave radiation: With increasing microwave intensity, the resonance peaks become smaller and side-peaks emerge. The distance between the central peak and the side-peaks is determined by the frequency of the radiation field which provides evidence for photon-assisted tunneling [16–19]. Photon-assisted tunneling through quantum dots is, in comparison to its counterpart in superconductor-insulator-superconductor junctions [53], a potentially richer phenomenon. The reason for this is that quantum dots form a multi-barrier structure which allows for real occupation and resonant tunneling. Therefore, a theoretical description requires to also take into account the influence of the field on the dynamics of the electrons localized in the central region between the barriers. The quantum dot setup used for the observation of photon-assisted tunneling can also be employed as an implementation [54] of the theoretically suggested non-adiabatic pump [37, 55, 56]. Lately, coupled quantum dots are frequently discussed in the context of quantum computation. They offer several possibilities to implement qubits and quantum logical gates, e.g. with the spin degree of freedom of an excess electron [57] or its position [58, 59].

Related experiments have been performed also with single quantum dots exposed to laser pulses which resonantly couple the highest occupied orbital and the lowest unoccupied orbital of the quantum dot [60]. Such a pulse can create an electron-hole pair which in turn is transformed by a transport voltage into a current pulse. Depending on their duration, pulses may not only excite an electron but also coherently de-excite the electron and thereby reduce the resulting current [61]. In the ideal case, the electron-hole pair is excited with probability unity and finally yields a dc current consisting of exactly one electron per pulse. This effect might be employed for the realization of a current standard. At present, however, the deviations from the ideal value of the current are still of the order of a few percent.

Molecular wires

During the last years, it became possible to adsorb organic molecules via thiol groups to a metallic gold surface. Thereby a stable contact between the molecule and the gold is established. This enables reproducible measurements of the current not only through artificial but also through real molecules. Single molecule conductance can be achieved in essentially two ways: One possible setup is an open break junction bridged by a molecule [1, 3, 62]. This setup can be kept stable for several hours. Moreover, it provides evidence for *single* molecule conductance because asymmetries in the current-voltage characteristics reflect asymmetries of the molecule [3, 63]. Alternatively, one can use a gold substrate as a contact and grow a self-assembled monolayer of molecules on it. The other contact is provided by a gold cluster on top of a scanning tunneling microscope tip which contacts one or a few molecules on the substrate [2, 64]. Naturally, the experimental effort with such molecular wires is accompanied by a vivid theoretical interest [4, 5, 13].

Typical energy scales of molecules lie in the infrared regime where most of today's lasers work. Hence, lasers represent a natural possibility to excite the electrons of the molecular wire and, thus, to study the corresponding changes of the conduction properties. At present, such experiments are attempted, but still no clearcut effect has been reported. The molecule-lead contacts seem stable even against relatively intense laser fields, but a main problem is the exclusion of side effects like, e.g. heating of the break junction which might distort the molecule-tip setup and, thus, be responsible for the observed enhancement of the conductance [65].

1.2 Wire-lead model

As a working model, we employ the externally driven transport setup of the type sketched in Fig. 1.1. Formally, it is described by the time-dependent wire-lead Hamiltonian

$$H(t) = H_{\rm wire}(t) + H_{\rm leads} + H_{\rm contacts}, \tag{1.1}$$

where the different terms correspond to the nanoscale conductor ("wire"), the leads, and the wire-lead couplings, respectively. We focus on the regime of coherent quantum transport where the main physics at work occurs on the wire itself. In doing so, we neglect other possible influences originating from driving induced hot electrons in the leads, dissipation on the wire and, as well, electron-electron interaction effects. Then, the wire Hamiltonian in a tight-binding approximation with N orbitals $|n\rangle$ reads

$$H_{\rm wire}(t) = \sum_{n,n'} H_{nn'}(t) c_n^\dagger c_{n'} \ . \tag{1.2}$$

For a molecular wire, this constitutes the so-called Hückel description where each site corresponds to one atom. The fermion operators c_n, $c_n^\dagger$ annihilate and create, respectively, an electron in the orbital $|n\rangle$. The influence of an applied ac field with frequency $\Omega = 2\pi/\mathcal{T}$

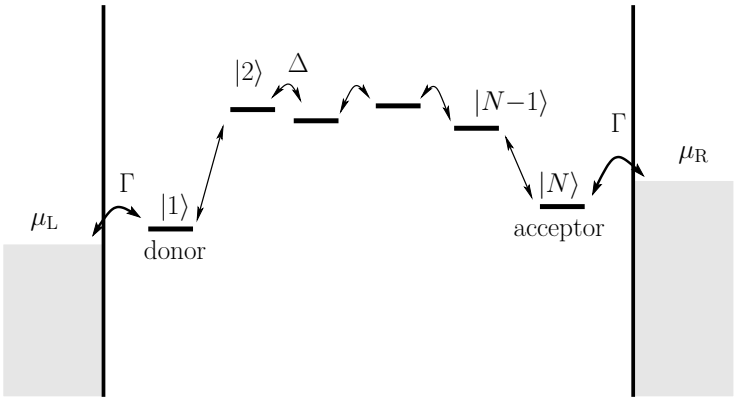

Figure 1.1: Level structure of a nano-conductor with $N = 6$ orbitals. The end sites, the so-called donor and acceptor, are coupled to two leads with chemical potentials μ_L and $\mu_R = \mu_L + eV$.

results in a periodic time dependence of the wire Hamiltonian, $H_{nn'}(t + \mathcal{T}) = H_{nn'}(t)$. The leads are modeled by ideal electron gases,

$$H_{\text{leads}} = \sum_q \epsilon_q (c^\dagger_{Lq} c_{Lq} + c^\dagger_{Rq} c_{Rq}), \tag{1.3}$$

where $c^\dagger_{Lq}$ ($c^\dagger_{Rq}$) creates an electron in the state $|Lq\rangle$ ($|Rq\rangle$) in the left (right) lead and q denotes to quantum numbers of the lead electrons. The tunneling Hamiltonian

$$H_{\text{contacts}} = \sum_q \left(V_{Lq} c^\dagger_{Lq} c_1 + V_{Rq} c^\dagger_{Rq} c_N \right) + \text{h.c.} \tag{1.4}$$

establishes the contact between the sites $|1\rangle$, $|N\rangle$ and the respective lead. This tunneling coupling is described by the spectral density

$$\Gamma_\ell(\epsilon) = 2\pi \sum_q |V_{\ell q}|^2 \delta(\epsilon - \epsilon_q) \tag{1.5}$$

of lead $\ell = L, R$ which becomes a smooth function if the lead modes are dense. If the leads are modeled by a tight-binding lattice, the $\Gamma_\ell(\epsilon)$ assume a semi-elliptic shape, the so-called Newns-Anderson density of states [66], which is sometimes employed in the context of molecular conduction [9, 67, 68]. Within the present context, however, we are mainly interested in the influence of the driving field on the conductor and not in the details of the coupling to the leads. Therefore, we choose for $\Gamma_\ell(\epsilon)$ a rather generic form by assuming that in the relevant regime, it is practically energy-independent,

$$\Gamma_\ell(\epsilon) \longrightarrow \Gamma_\ell. \tag{1.6}$$

Thus, all explicit results presented herein are evaluated within this so-called wide-band limit.

In order to fully specify the dynamics, we choose as an initial condition for the left/right lead a grand-canonical electron ensemble at temperature T and electro-chemical potential

$\mu_{L/R}$, respectively. Thus, we assume at initial time t_0 the density matrix

$$\varrho_0 \propto e^{-(H_{\rm leads}-\mu_L N_L-\mu_R N_R)/k_B T}, \tag{1.7}$$

where $N_\ell = \sum_q c_{\ell q}^\dagger c_{\ell q}$ is the number of electrons in lead ℓ and k_B denotes the Boltzmann constant. An applied voltage V corresponds to a chemical potential difference $\mu_R - \mu_L = eV$ with $-e$ being the electron charge. Then, at t_0, the only nontrivial expectation values of the wire operators read $\langle c_{\ell' q'}^\dagger c_{\ell q}\rangle = \delta_{\ell\ell'}\delta_{qq'} f_\ell(\epsilon_q)$, where $f_\ell(\epsilon) = (1+\exp[(\epsilon-\mu_\ell)/k_B T])^{-1}$ denotes the Fermi function.

Below, we specify the wire Hamiltonian as a tight-binding model composed of N sites as sketched in Fig. 1.1. Each orbital is coupled to its nearest neighbor by a hopping matrix element Δ, thus, the single-particle wire Hamiltonian reads

$$\mathcal{H}_{\rm wire}(t) = -\Delta \sum_{n=1}^{N-1} \big(|n\rangle\langle n{+}1| + |n{+}1\rangle\langle n|\big) + \sum_n [E_n + x_n\, a(t)]\, |n\rangle\langle n|, \tag{1.8}$$

where E_n denote the on-site energies of the tight-binding levels. Although the theoretical approach derived below is valid for an arbitrary periodically driven wire Hamiltonian, we always assume that the time dependence results from the coupling to an oscillating dipole field that causes the time-dependent level shifts $x_n a(t)$, where $x_n = (N{+}1{-}2n)/2$ denotes the scaled position of site $|n\rangle$. The energy $a(t) = a(t+\mathcal{T})$ is determined by the electrical field strength multiplied by the electron charge and the distance between two neighboring sites.

We assume that the wire couples equally strong to both leads, thus, $\Gamma_L = \Gamma_R \equiv \Gamma$. An applied transport voltage V is mapped to a symmetric shift of the leads' chemical potentials, $\mu_R = -\mu_L = eV/2$. Moreover, for the evaluation of the dc current and the zero-frequency noise, we restrict ourselves to zero temperature. The zero-temperature limit is physically well justified for molecular wires at room temperature and for quantum dots at helium temperature since in both cases thermal electron excitations do not play a significant role.

In a realistic wire molecule, Δ is of the order 0.1 eV. Thus, a typical wire-lead hopping rate $\Gamma = 0.1\Delta$ yields $e\Gamma/\hbar = 2.56 \times 10^{-5}$ Ampère and $\Omega \approx 10\Delta/\hbar$ corresponds to a laser frequency in the near infrared and to wavelengths of the order 1 μm. For a typical distance of 5Å between two neighboring sites, a driving amplitude $A = \Delta$ is equivalent to an electrical field strength of 2×10^6 V/cm. It must be emphasized that the amplitude A is determined by the local electrical field between the contacts. The difference to the incident field can be huge: Model calculations demonstrated that the presence of metallic tips enhances the local field by several orders of magnitude [69, 70]. This explains the observation that the Raman scattering intensity increases drastically once the molecules are adsorbed to a metallic surface [71, 72]. Coupled quantum dots typically [15, 16, 18] have a distance of less than 1 μm while the coupling matrix element Δ is of the order of 30 μeV which corresponds to a wavelength of roughly 1 cm. The dipole approximation inherent to the time-dependent part of the Hamiltonian (1.8) neglects the propagation of the electromagnetic field and, thus, is valid only for wavelengths that are much larger than the size of the sample [73]. This condition is indeed fulfilled for both applications we have in mind.

1.3 Transport theory

1.3.1 Tien-Gordon theory

In order to explain the steps in the current-voltage characteristics of microwave-irradiated superconductor-insulator-superconductor junctions [53], Tien and Gordon [74] proposed a heuristical theoretical treatment which is of appealing simplicity but nevertheless captures some essential features of driven transport. The central idea of this approach is to model the influence of the driving fields by a periodic shift of the energies in the, e.g. left lead according to

$$\tilde{\epsilon}_{Lq}(t) = \epsilon_{Lq} + A\cos(\Omega t). \tag{1.9}$$

Then the corresponding lead eigenstates evolve as

$$|Lq\rangle_t = \exp\Big(-\frac{\mathrm{i}}{\hbar}\epsilon_{Lq}t - \mathrm{i}\frac{A}{\hbar\Omega}\sin(\Omega t)\Big)|Lq\rangle \tag{1.10}$$

$$= \sum_{k=-\infty}^{\infty} J_k(A/\hbar\Omega)\exp\Big(-\frac{\mathrm{i}}{\hbar}(\epsilon_{Lq} + k\hbar\Omega)t\Big)|Lq\rangle, \tag{1.11}$$

where J_k denotes the kth order Bessel function of the first kind. The interpretation of the Fourier decomposition (1.11) is that each state consists of sidebands whose energies are shifted by multiples of $\hbar\Omega$. For the evaluation of the dc current, this is equivalent to replacing the Fermi function of the left lead by

$$f_L(E) \longrightarrow \sum_k J_k^2(A/\hbar\Omega) f_L(E + k\hbar\Omega) \tag{1.12}$$

and formally treating the system as time-independent [74]. While this effective static treatment indeed captures the photon-assisted dc current, it naturally fails to describe the ac response.

For time-dependent wire-lead models where the driving shifts all wire levels simultaneously, it is possible to map the driving field by a gauge transformation to oscillating chemical potentials. Then, the average current can be evaluated from an effective electron distribution like the one in Eq. (1.12) [75–77]. However, generally the time-dependent field also influences the dynamics of the electrons on the wire. In particular, this is the case for the dipole driving (1.8). Then, a treatment beyond Tien-Gordon theory becomes necessary. Deriving an approach which is valid in the general case is the objective of Chap. 2.

1.3.2 Scattering approach for static conductors

In the absence of a driving field, the computation of the coherent transport through mesoscopic structures has become a standard procedure [26–29]. The crucial idea goes back to Landauer who postulated already in 1957 [25] that in the absence of both inelastic effects and electron-electron interaction, conduction can be described as a coherent scattering

process of independent electrons. Then, an infinitesimal voltage V causes the current $I = GV$ with the (linear) conductance

$$G = \frac{e^2}{h}T, \tag{1.13}$$

of a one-dimensional conductor, where T is the transmission probability of an electron at the Fermi surface. Since conductors may have non-vanishing reflection probability $1 - T$, the transmission does not necessarily assume an integer value. The prefactor $e^2/h = (25.8\,\mathrm{k\Omega})^{-1}$ is the so-called conductance quantum.

Originally [25], the conductance (1.13) has been proposed with T replaced by $T/(1-T)$. In the beginning of the 1980's, there has been a theoretical debate [78–80] whether or not, the reflection coefficient $1 - T$ has to be included. The controversy was resolved by considering four-terminal devices where two terminals act as voltage probes and are considered as a part of the mesoscopic conductor [81, 82]. Then, V represents the probed voltage and the factor $1/(1 - T)$ indeed is justified. In a two-terminal device, however, V denotes the externally applied voltage and the conductance includes a contact resistance and is given by Eq. (1.13).

With the same ideas, Landauer theory can be generalized to the case of a finite voltage for which the current reads

$$I = \frac{e}{h}\int \mathrm{d}E\,\big[f_R(E) - f_L(E)\big]T(E), \tag{1.14}$$

with $T(E)$ the electron transmission at energy E. The electron distribution in the left (right) lead is given by the Fermi function $f_{L(R)}$ with the chemical potential $\mu_{L(R)}$ whose difference $\mu_L - \mu_R = eV$ is determined by the applied voltage. Linearization for small voltages yields the conductance (1.13). The current formula (1.14) and the conductance (1.13) have been derived from Kubo formula [79–81, 83, 84] and non-equilibrium Green functions [85–87] for various microscopic models. In doing so, one usually starts by defining a current operator, e.g. as the change of the electron charge eN_L in the left lead, i.e. $I = \mathrm{i}e[H, N_L]/\hbar$. Finally, one obtains the expected expression for the current together with a relation between the transmission $T(E)$ and the Green function of the electrons.

In order to obtain an expression for the related current noise, one considers the symmetrized correlation function

$$S(t, t') = \frac{1}{2}\big\langle[\Delta I(t), \Delta I(t')]_+\big\rangle \tag{1.15}$$

of the current fluctuation operator $\Delta I(t) = I(t) - \langle I(t)\rangle$, where the anticommutator $[A, B]_+ = AB + BA$ ensures hermiticity. For a stationary process, the correlation function $S(t, t') = S(t - t')$ is a function of only the time difference. Then, the noise strength can be characterized by the zero-frequency component

$$S = \int_{-\infty}^{\infty} \mathrm{d}\tau\, S(\tau), \tag{1.16}$$

which obeys $S \geq 0$ according to the Wiener-Khinchine theorem. In terms of the transmission function $T(E)$, the noise strength S reads [30]

$$\begin{aligned} S = \frac{e^2}{h} \int \mathrm{d}E \Big\{ & T(E)\big[f_L(E)[1-f_L(E)] + f_R(E)[1-f_R(E)]\big] \\ & + T(E)\big[1-T(E)\big]\big[f_R(E)-f_L(E)\big]^2 \Big\}. \end{aligned} \tag{1.17}$$

A dimensionless measure for the *relative* noise strength, is the so-called Fano factor [88]

$$F = \frac{S}{e|I|}\,. \tag{1.18}$$

Note that in a two-terminal device, both the absolute value of the average current and the noise strength are independent of the contact ℓ. Historically, the zero-frequency noise (1.16) contains a factor 2, i.e., one considers $S' = 2S$, resulting from a different definition of the Fourier transform. Then, the Fano factor is defined as $F = S'/2e|I|$. The definition (1.18) is such that a Poisson process corresponds to $F = 1$.

The generalization of the noise expression (1.17) to driven systems must also account for absorption and emission. Owing to this energy non-conserving processes, the zero-frequency noise is no longer given solely in terms of transmission *probabilities* but also depends on the phases of the transmission *amplitudes* [A5, A9, 40]; cf. Eq. (2.19), below.

1.3.3 Master equation

A different strategy for the computation of stationary currents relies on the derivation of a master equation for the dynamics of the wire electrons. There, the central idea is to consider the contact Hamiltonian (1.4) as a perturbation, while the dynamics of the leads and the wire, including the external driving, is treated exactly. From the Liouville-von Neumann equation $\mathrm{i}\hbar\dot{\varrho}(t) = [H(t), \varrho(t)]$ for the total density operator $\varrho(t)$ one obtains by standard techniques [89, 90] the approximate equation of motion

$$\begin{aligned} \dot{\varrho}(t) = & -\frac{\mathrm{i}}{\hbar}[H_{\mathrm{wire}}(t) + H_{\mathrm{leads}}, \varrho(t)] \\ & - \frac{1}{\hbar^2}\int_0^\infty \mathrm{d}\tau [H_{\mathrm{contacts}}, [\widetilde{H}_{\mathrm{contacts}}(t-\tau, t), \varrho(t)]]. \end{aligned} \tag{1.19}$$

The tilde denotes operators in the interaction picture with respect to the molecule and the lead Hamiltonian without the molecule-lead coupling, $\widetilde{X}(t,t') = U_0^\dagger(t,t')\, X\, U_0(t,t')$, where U_0 is the propagator without the coupling. For the evaluation of Eq. (1.19) it is essential to use an exact expression for the zeroth-order time evolution operator $U_0(t,t')$. The use of any approximation bears the danger of generating artifacts, which, for instance, may lead to a violation of fundamental equilibrium properties [91, 92] as discussed in Sec. 2.1.2.

In order to make practical use of equation (1.19), one has to trace over the lead degrees of freedom and thereby obtains a master equation for the reduced density operator of the wire electrons. Subsequently, the reduced density operator is decomposed into the eigenstates of the wire Hamiltonian H_{wire}—or the corresponding Floquet states (2.2) if

the system is driven. As a further simplification, one might neglect off-diagonal matrix elements and, thus, obtain a master equation of the Pauli type, i.e., a closed equation for the occupation *probabilities* of the eigenstates [56, 93, 94]. For driven systems close to degeneracies of the quasienergies, however, such a Pauli master equation is not reliable as has been exemplified in Ref. [A10].

2 Floquet transport theory

Floquet theory represents a proper tool for the treatment of periodically driven systems. Originally developed for ordinary differential equations [95], it has been adapted to the case of purely coherent quantum dynamics [96–98], scattering theory [32, 33], dissipative quantum mechanics [99–102], and also classical Brownian motion [103]. Of specific interest in the present context are methods that combine Floquet theory with the established transport theories presented in the introduction [56, 104]. This chapter reviews contributions by the present author to these approaches. In particular, a Floquet master equation approach [A4, A10], a Floquet scattering theory [A9], and a high-frequency approximation scheme [A6, A9] are discussed.

2.1 Floquet master equation approach

For a perturbative treatment of the wire-lead coupling in a transport problem, one conveniently starts from the master equation (1.19) which depends implicitly via the interaction picture operator with respect to the uncoupled subsystems on the dynamics of the electrons on the isolated wire. Therefore, the solution of the master equation requires knowledge of the electron dynamics in the driven wire in the absence of the leads. This will be calculated with the help of Floquet theory. A clear advantage of this approach is the possibility to directly include phonon damping. A drawback is its restriction to weak and intermediate wire-lead couplings. The master equation presented below goes beyond the one of Ref. [94] in two respects: Firstly, it contains also off-diagonal elements of the reduced density matrix which in some cases are essential [A10]. Secondly, in a further step, the master equation is extended to the case of phonon damping. This brings about an effective electron-electron interaction and renders the master equation non-linear.

2.1.1 Coherent transport

At a first stage, we focus on coherent[1] transport and derive an expression for the ac current defined as the net (incoming minus outgoing) electrical current through the left contact. It is given by minus the time-derivative of the electron number in the left lead multiplied by the electron charge $-e$, $I_L(t) = e(\mathrm{d}/\mathrm{d}t)\langle N_L\rangle$. From the master equation (1.19) follows in the wide-band limit the expression

$$\begin{aligned} I_L(t) &= e\,\mathrm{tr}[\dot{\varrho}(t)N_L] \\ &= \frac{e}{\hbar}\Gamma_L\big\langle c_1^\dagger c_1\big\rangle - e\frac{\Gamma_L}{\pi\hbar^2}\,\mathrm{Re}\int_0^\infty \mathrm{d}\tau \int \mathrm{d}\epsilon\, \mathrm{e}^{\mathrm{i}(\epsilon+\mu_L)\tau/\hbar} f(\epsilon)\big\langle [c_1, \tilde{c}_1^\dagger(t-\tau,t)]_+\big\rangle. \end{aligned} \tag{2.1}$$

[1] In this context, the term "coherent" refers to the dynamics of single electrons in the entire wire-lead setup in the absence of phonon damping.

and *mutatis mutandis* for the net current through the right contact. Equation (2.1) expresses the current by the expectation values $\langle[c_n, \tilde{c}_n(t-\tau,t)]_+\rangle$ and $\langle c_1^\dagger c_1\rangle$. We emphasize that these quantities depend on the dynamics of the isolated wire and are thus influenced by the driving via the interaction picture operator $c_1^\dagger(t-\tau,t)$.

Floquet decomposition

In order to gain an explicit expression for $\tilde{c}_1$, we focus on the driven molecule decoupled from the leads. Since its Hamiltonian is periodic in time, $H_{nn'}(t) = H_{nn'}(t+\mathcal{T})$, $\mathcal{T} = 2\pi/\Omega$, we can solve the time-dependent Schrödinger equation within a Floquet approach, i.e., we make use of the fact that there exists a complete set of solutions of the form

$$|\psi_\alpha(t)\rangle = e^{-\mathrm{i}\epsilon_\alpha t/\hbar}|\phi_\alpha(t)\rangle \tag{2.2}$$

with the quasi-energies ϵ_α. The so-called Floquet states $|\phi_\alpha(t)\rangle$ obey the time-periodicity of the driving field and, thus, can be decomposed into a Fourier series,

$$|\phi_\alpha(t)\rangle = \sum_{k=-\infty}^{\infty} e^{-\mathrm{i}k\Omega t}|\phi_{\alpha,k}\rangle. \tag{2.3}$$

Moreover, the Floquet states fulfill the quasienergy equation [96, 97, 101, 102, 105]

$$\Big(\mathcal{H}(t) - \mathrm{i}\hbar\frac{\mathrm{d}}{\mathrm{d}t}\Big)|\phi_\alpha(t)\rangle = \epsilon_\alpha|\phi_\alpha(t)\rangle, \tag{2.4}$$

where $\mathcal{H}(t) = \sum_{n,n'}|n\rangle H_{nn'}(t)\langle n'|$ denotes the single-particle Hamiltonian (1.8) of the wire electrons. A wealth of methods for the solution of this eigenvalue problem can be found in the literature [101, 105]. Among them are the numerical diagonalization of the operator on left-hand side of eigenvalue equation (2.4), propagation schemes [106], perturbation theory [50, 97, 107], and matrix-continued fraction schemes [105, 108].

To make use of the knowledge about the driven molecule that we obtain from Floquet theory, we define the Floquet representation of the fermionic creation and annihilation operators by the time-dependent transformation

$$c_\alpha(t) = \sum_n \langle\phi_\alpha(t)|n\rangle\, c_n, \tag{2.5}$$

$$c_n = \sum_\alpha \langle n|\phi_\alpha(t)\rangle\, c_\alpha(t). \tag{2.6}$$

The back transformation (2.6) follows from the mutual orthogonality and the completeness of the Floquet states at equal times [101]. It is now straightforward to prove that $\tilde{c}_\alpha(t-\tau,t) = c_\alpha(t)\exp(\mathrm{i}\epsilon_\alpha\tau/\hbar)$. Technically, the separation of the times t and τ is crucial because it enables the evaluation of the corresponding time and energy integrations. Averaging $I_L(t)$ over the driving period yields the dc current

$$\bar{I} = -\frac{e\Gamma_L}{\hbar}\sum_{\alpha k}\Big[\langle\phi_{\alpha,k}|1\rangle\langle 1|\phi_{\alpha,k}\rangle f_L(\epsilon_\alpha + k\hbar\Omega) - \sum_{\beta k'}\langle\phi_{\alpha,k'+k}|1\rangle\langle 1|\phi_{\beta,k'}\rangle R_{\alpha\beta,k}\Big], \tag{2.7}$$

where $R_{\alpha\beta}(t) = \langle c_\beta^\dagger(t) c_\alpha(t)\rangle = \sum_k \mathrm{e}^{-\mathrm{i}k\Omega t} R_{\alpha\beta,k}$ denotes the single-particle density operator in the Floquet basis. We have used the fact that the $R_{\alpha\beta}(t)$ are expectation values of a dissipative, periodically driven system. Therefore, in the long-time limit, they share the time-periodicity of the driving field and, consequently, the long-time limit of $R_{\alpha\beta}(t)$ can be represented by a Fourier series.

Reduced master equation in Floquet basis

The remaining task in computing the stationary current is to find the Fourier coefficients $R_{\alpha\beta,k}$ at asymptotic times. For that purpose, we derive a master equation for the $R_{\alpha\beta}(t)$ from Eq. (1.19) by tracing out the leads' degrees of freedom followed by inserting the Floquet decomposition (2.6) for the wire operators. Since all coefficients of this master equation as well as its asymptotic solution are $\mathcal{T}$-periodic, we can split it into its Fourier components. Finally, we obtain for the $R_{\alpha\beta,k}$ the inhomogeneous set of equations

$$\begin{aligned}
\mathrm{i}(\epsilon_\alpha - \epsilon_\beta + k\hbar\Omega) R_{\alpha\beta,k} = \frac{\Gamma_L}{2} \sum_{k'} \Big\{ & \sum_{\beta' k''} \langle \phi_{\beta,k''+k'}|1\rangle\langle 1|\phi_{\beta',k''+k}\rangle R_{\alpha\beta',k'} \\
& + \sum_{\alpha' k''} \langle \phi_{\alpha',k''+k'}|1\rangle\langle 1|\phi_{\alpha,k''+k}\rangle R_{\alpha'\beta,k'} \\
& - f_L(\epsilon_\alpha + k'\hbar\Omega)\langle \phi_{\beta,k'-k}|1\rangle\langle 1|\phi_{\alpha,k'}\rangle \\
& - f_L(\epsilon_\beta + k'\hbar\Omega)\langle \phi_{\beta,k'}|1\rangle\langle 1|\phi_{\alpha,k'+k}\rangle \Big\} \\
& + \text{same terms with the replacement } (L,1) \leftrightarrow (R,N).
\end{aligned} \tag{2.8}$$

For the typical parameter values used below, a large number of sidebands contributes significantly to the Fourier decomposition of the Floquet modes $|\phi_\alpha(t)\rangle$. Numerical convergence for the solution of the master equation (2.8), however, is already obtained by using a few sidebands for the decomposition of $R_{\alpha\beta}(t)$. This keeps the numerical effort relatively small and justifies the use of the Floquet representation (2.6). It enables to treat the problem beyond the usual rotating-wave-approximation [94]. In certain parameter regimes, avoiding a rotating-wave approximation indeed turns out to be crucial [A10].

2.1.2 Phonon damping

In order to describe the electron transport under the influence of phonon damping, commonly a bosonic heat bath is coupled to each wire site, which renders the on-site energies fluctuating with quantum noise [10–12, 109–119]. This can be considered as an extension of the spin-boson model to more than two sites and the presence of leads. For the master equation (1.19), one then has in the first line in addition the Hamiltonian of the phonon bath, while the electron-phonon coupling enters as a further dissipative contribution to the second line. Note that this leaves the current (2.1) formally unchanged.

When evaluating the master equation, however, it turns out that in addition to the terms containing the single-electron density matrix $R_{\alpha\beta}(t)$, two-electron expectation values of the form $\langle c_\delta^\dagger\, c_\gamma^\dagger\, c_\beta\, c_\alpha\rangle_t$ appear. By iteration, one thus generates a hierarchy of equations

up to N-electron expectation values. To obtain a description in terms of only the single-electron expectation values, we employ the Hartree-Fock decoupling scheme defined by the approximation

$$\langle c_\delta^\dagger\, c_\gamma^\dagger\, c_\beta\, c_\alpha\rangle \approx \langle c_\delta^\dagger\, c_\alpha\rangle\langle c_\gamma^\dagger\, c_\beta\rangle - \langle c_\delta^\dagger\, c_\beta\rangle\langle c_\gamma^\dagger\, c_\alpha\rangle = R_{\alpha\delta}R_{\beta\gamma} - R_{\beta\delta}R_{\alpha\gamma}. \tag{2.9}$$

Clearly, such a mean-field approximation only covers certain aspects of the full many-particle problem. Nevertheless, it offers a feasible and consistent description. As a most striking consequence, the Hartree-Fock decoupling (2.9) makes the master equation non-linear.

Thermal equilibrium

A potential problem of quantum master equations has been pointed out in Refs. [91,120], namely that they might not be consistent with the second law of thermodynamics—in particular, that they might not predict zero current even in the absence of both transport voltage and driving. This apparent lack of a proper equilibrium limit, however, is not inherent to master equations of the form (1.19) themselves, but results from an inconsistent treatment at a later stage: It is crucial to employ in the second line of Eq. (1.19) the *exact* interaction picture operators of the uncoupled subsystems. Using any approximation indeed bears the danger of inconsistencies. Master equations whose equilibrium limit suffer from the mentioned problems, have, e.g. been derived in Ref. [121] and applied to non-equilibrium situations with a finite transport voltage [54, 55] and with time-dependent fields [112, 122] where no contradiction occurs.

Therefore, an important consistency check for quantum master equations is an equilibrium situation, where $H_{nn'}$ is time-independent and where no external bias is present ($\mu_\ell = \mu$ for all ℓ). It can be demonstrated [A10] that our final reduced master equation (2.8) in the absence of both driving and voltage has the solution $R_{\alpha\beta} = \delta_{\alpha\beta} f_\alpha$, with the population $f_\alpha = f(E_\alpha - \mu)$, determined by the Fermi distribution and the energy E_α of the eigenstates $|\phi_\alpha\rangle$ which represent the undriven limit of the Floquet states. Consequently, the current (2.7) vanishes in accordance with elementary principles of statistical physics.

2.2 Floquet scattering approach

Since the Hamiltonian (1.1) is bilinear in the creation and the annihilation operators, the Heisenberg equations for these operators are linear. Thus, in the absence of phonon damping, the transport problem can be solved exactly. Here, we present such an exact solution which also makes use of a Floquet ansatz. However, then the Floquet equation (2.4) becomes non-hermitian due to the presence of an imaginary self-energy contribution. As a drawback, this exact Floquet treatment cannot be extended directly to situations that include strong electron-electron correlations or phonon damping. We derive explicit expressions for the current and the noise strength only for the wide-band limit (1.6). For a formulation beyond this limit and for the details of the calculation, the reader is referred to Ref. [A9]. Related approaches have been presented which, however, are perturbative in the driving Hamiltonian, [123–125] or do not obtain a "scattering form" for the current [36,37].

Floquet ansatz for the propagator

For the retarded Green function of the wire electrons, one finds, after eliminating the leads, the equation of motion [A5]

$$\Big(\mathrm{i}\hbar\frac{\mathrm{d}}{\mathrm{d}t} - \mathcal{H}(t) + \mathrm{i}\Sigma\Big)G(t,t') = \delta(t-t'), \tag{2.10}$$

where $\mathcal{H}(t) = \sum_{n,n'} |n\rangle H_{nn'}(t)\langle n'|$ and $2\Sigma = |1\rangle\Gamma_L\langle 1| + |N\rangle\Gamma_R\langle N|$ is the self-energy which results from the coupling to the leads. For the current which is again defined as the change of the charge in the, e.g. left lead, $I_L = e(\mathrm{d}/\mathrm{d}t)\langle N_L\rangle$, we find after some algebra that it assumes the commonly expected "scattering form" [27] but with periodically *time-dependent* transmission probabilities. In addition, we obtain a contribution that accounts for a $\mathcal{T}$-periodic charging and discharging of the wire [A5,A9] which vanishes in the average over one driving period. Here, we restrict ourselves to the time-averaged current

$$\bar{I} = \frac{e}{h}\sum_{k=-\infty}^{\infty}\int \mathrm{d}\epsilon\,\big\{T_{LR}^{(k)}(\epsilon)f_R(\epsilon) - T_{RL}^{(k)}(\epsilon)f_L(\epsilon)\big\}. \tag{2.11}$$

$T_{LR}^{(k)}(\epsilon) = \Gamma_L\Gamma_R|G_{1N}^{(k)}(\epsilon)|^2$ denotes the transmission of an electron with energy ϵ from the right lead to the left lead under the absorption (emission) of $|k|$ photons if $k > 0$ ($k < 0$) and $T_{RL}^{(k)}(\epsilon)$ accordingly. $G_{1N}^{(k)}(\epsilon)$ denotes the relevant matrix elements of the Fourier transform of the retarded Green function

$$G^{(k)}(\epsilon) = \frac{1}{\mathcal{T}}\int_0^{\mathcal{T}} \mathrm{d}t\,\mathrm{e}^{\mathrm{i}k\Omega t}\int_{-\infty}^{+\infty}\mathrm{d}\tau\,\mathrm{e}^{\mathrm{i}\epsilon\tau/\hbar}\,G(t,t-\tau). \tag{2.12}$$

Note that, consistent with Ref. [34], no "Pauli blocking factors" $1 - f_\ell$ appear in the current formula (2.11). In contrast to a static situation, this is of relevance here since for a driven system $T_{LR}^{(k)}(\epsilon)$ and $T_{RL}^{(k)}(\epsilon)$ are in general unrelated. Since the coefficients of the equation of motion (2.10) are $\mathcal{T}$-periodic, a complete solution can be constructed with the help of the Floquet ansatz

$$|\psi_\alpha(t)\rangle = \exp[(-\mathrm{i}\epsilon_\alpha/\hbar - \gamma_\alpha)\,t]\,|u_\alpha(t)\rangle \tag{2.13}$$

which differs from (2.2) by the imaginary part $-\mathrm{i}\hbar\gamma_\alpha$ of the quasienergies. Like in the coherent case, the Floquet states

$$|u_\alpha(t)\rangle = \sum_k |u_{\alpha k}\rangle\exp(-\mathrm{i}k\Omega t) \tag{2.14}$$

obey the time-periodicity of the Hamiltonian. In a Hilbert space that is extended by a periodic time coordinate, they fulfill the Floquet eigenvalue equation

$$\Big(\mathcal{H}(t) - \mathrm{i}\Sigma - \mathrm{i}\hbar\frac{\mathrm{d}}{\mathrm{d}t}\Big)|u_\alpha(t)\rangle = (\epsilon_\alpha - \mathrm{i}\hbar\gamma_\alpha)|u_\alpha(t)\rangle. \tag{2.15}$$

Since the eigenvalue equation (2.15) is non-hermitian, its eigenvalues $\epsilon_\alpha - \mathrm{i}\hbar\gamma_\alpha$ are generally complex valued and the (right) eigenvectors are not mutually orthogonal. Therefore, we

need to solve also the adjoint Floquet equation yielding again the same eigenvalues but providing the adjoint eigenvectors $|u_\alpha^+(t)\rangle$. Thus, we find the retarded Green function

$$G(t,t-\tau) = -\frac{\mathrm{i}}{\hbar}\sum_\alpha |\psi_\alpha(t)\rangle\langle\psi_\alpha^+(t-\tau)|\,\Theta(\tau) = G(t+\mathcal{T},t+\mathcal{T}-\tau) \tag{2.16}$$

and, consequently,

$$G_{nn'}^{(k)}(\epsilon) = \sum_{\alpha,k'} \frac{\langle n|u_{\alpha,k'+k}\rangle\langle u_{\alpha,k'}^+|n'\rangle}{\epsilon-(\epsilon_\alpha+k'\hbar\Omega-\mathrm{i}\hbar\gamma_\alpha)}. \tag{2.17}$$

The current noise is given by the symmetrized auto-correlation function (1.15) of the current fluctuation operator $\Delta I(t) = I(t) - \langle I_L(t)\rangle$. It can be shown that after the decay of all transients, $S(t,t') = S(t+\mathcal{T},t'+\mathcal{T})$. Therefore, it is possible to characterize the noise level by the time-averaged zero-frequency noise,

$$\bar{S} = \frac{1}{\mathcal{T}}\int_0^{\mathcal{T}} \mathrm{d}t \int_{-\infty}^{\infty} \mathrm{d}\tau\, S_L(t,t-\tau) \tag{2.18}$$

which differs from the static case by a time average, cf. Eq. (1.15). Since the total charge is conserved, the noise strength is independent of whether the current is defined via the electron number in the left lead or in the right lead. After some algebra, one obtains [A5, A9]

$$\begin{aligned}\bar{S} = \frac{e^2}{h}\Gamma_L\Gamma_R \sum_k \int \mathrm{d}\epsilon \Big\{ &\Gamma_L\Gamma_R \Big| \sum_{k'} G_{N1}^{(k'-k)}(\epsilon_k)[G_{N1}^{(k')}(\epsilon)]^* \Big|^2 f_L(\epsilon)\bar{f}_L(\epsilon_k) \\ &+ \Big|\Gamma_L \sum_{k'} G_{1N}^{(k'-k)}(\epsilon_k)[G_{11}^{(k')}(\epsilon)]^* - \mathrm{i}G_{1N}^{(-k)}(\epsilon_k)\Big|^2 f_L(\epsilon)\bar{f}_R(\epsilon_k)\Big\} \\ &+ \text{same terms with the replacement } (L,1)\leftrightarrow(R,N),\end{aligned} \tag{2.19}$$

with $\bar{f}_{L/R} = 1 - f_{L/R}$ and $\epsilon_k = \epsilon + k\hbar\Omega$.

Expressions (2.11) and (2.19) contain prior findings as special cases: In the absence of any driving, the Floquet eigenvalues $\epsilon_\alpha - \mathrm{i}\hbar\gamma_\alpha$ reduce to the complex-valued eigenenergies; this implies $G_{nn'}^{(k)} = 0$ for all $k \neq 0$. Therefore, only the terms for $k = 0$ contribute and the the transmission probability for an electron with energy E becomes $T(E) = \Gamma_L\Gamma_R|G_{N1}^{(0)}(E)|^2$. Thus, the current and the noise in the static limit become the expressions (1.14) and (1.16), respectively [30]. In order to achieve an expression for the noise that depends only on the transmission probability $T(E)$, we simplified the second line of Eq. (2.19) using the relation $|\Gamma_L(\epsilon)G_{11}(\epsilon)+\mathrm{i}|^2 = 1-T(\epsilon)$ which is valid for undriven conductors [27]. Note that in contrast to the time-dependent case, the noise expression (2.19) cannot be brought into such a convenient form and, thus, generally depends on the phase of the transmission amplitude.

Related expressions for the noise have also been derived for the low-frequency ac conductance [38, 39] and the scattering by a slowly time-dependent potential [40]. For a system for which the ac potential is spatially uniform in the driven region, the average current and the noise strength follow in the low tunneling limit already from the static conduction properties within a Tien-Gordon-like approach [126, 127].

2.3 High-frequency approximation

Floquet theory is based on the eigenvalue equation (2.4) with the underlying structure of an extended Hilbert space [101]. Thus, it is possible to adapt methods known from the computation of eigenstates of a time-independent Hamiltonian, like Schrödinger perturbation theory, to the driven case [96, 97]. A perturbative treatment has been applied to driven tunneling in bistable potentials [49, 50, 128], to the motion of an electron in a superlattice [51, 107], and to the dynamics of two interacting electrons in a double quantum dot [52, 129]. After a brief introduction to this perturbative approach for fully coherent quantum systems, we describe an equivalent approach for quantum systems which are coupled to external degrees of freedom and discuss its application to transport problems [A6] and the corresponding treatment of driven dissipative quantum systems [A7].

Driven coherent quantum dynamics

Let us consider the special case of a time-dependent Hamiltonian of the form

$$H = H_0 + H_1\, a(t) \tag{2.20}$$

where $a(t)$ is a $\mathcal{T}$-periodic function with zero time-average. In order to derive an effective static description, we start out by applying the unitary transformation

$$U_0(t) = \exp\Big(-\frac{\mathrm{i}}{\hbar} H_1 \int_0^t \mathrm{d}t' a(t') \Big) \tag{2.21}$$

to the Hamiltonian (2.20) followed by replacing it by its time-average

$$\bar{H}_0 = \frac{1}{\mathcal{T}} \int_0^{\mathcal{T}} \mathrm{d}t\, U_0^\dagger(t) H_0 U_0(t). \tag{2.22}$$

Note that $U_0(t) = U_0(t+\mathcal{T})$, owing to the zero time-average of $a(t)$. In the limit of high driving frequencies, the static effective Hamiltonian (2.22) can be used for the description of the time-dependent system. It has been demonstrated in the appendix of Ref. [A6] that this heuristically introduced approximation is equivalent to a Schrödinger perturbation theory for the Floquet Hamiltonian (2.20) with $1/\Omega$ being a small parameter.

Electron transport through time-dependent systems

For a transport situation with the dipole driving we assign the time-dependent part of the time-dependent wire Hamiltonian (1.8) to $H_1\, a(t)$. From inserting the static part of (1.8) into Eq. (2.22), we obtain a renormalized wire Hamiltonian as in the case of an isolated quantum system.

A proper treatment of the wire-lead coupling Hamiltonian, however, is more involved. This becomes clear from the following consideration: The influence of the leads on the wire electrons can be subsumed into a Gaussian fluctuation operator with vanishing mean value and a correlation function which is determined by the Fermi distribution [A5, A6]. However, the fluctuation operator vanishes in the average over the driving period. Therefore,

one has to evaluate the correlation functions first and to perform a time-average at a later stage. Then one obtains an effective electron distribution as in the case of Tien-Gordon theory, cf. Sec. 1.3.1. The resulting *static* effective problem of course is much easier to handle and can often be treated analytically.

In order to give a specific example, we anticipate the results for the transport through a driven two-level system discussed in Ref. [A6]; cf. Chap. 5. For this example, the high-frequency approximation scheme results in a renormalization of the tunnel matrix element between the two sites, Δ, and an effective electron distribution, i.e.,

$$\Delta \longrightarrow \Delta_{\text{eff}} = J_0(A/\hbar\Omega)\Delta, \tag{2.23}$$

$$f_\ell(\epsilon) \longrightarrow f_{\text{eff}}(\epsilon) = \sum_k J_k^2(A/2\hbar\Omega) f_\ell(\epsilon + k\hbar\Omega), \quad \ell = L, R \tag{2.24}$$

where J_k denotes the kth order Bessel function of the first kind and A and Ω are the driving amplitude and frequency, respectively. Note that the argument of the Bessel function depends on the specific definition of the driving amplitude, which explains the difference to Eq. (1.12). The effective electron distribution could have been obtained also within a Tien-Gordon-like approach, while the renormalization of the tunnel matrix element is (i) beyond Tien-Gordon and (ii) is essential for the agreement with the exact numerical results [A6].

Dissipative quantum mechanics

Although we here focus on the electron transport between two leads, it is worth mentioning that the ideas presented in this subsection can also be applied to driven quantum systems coupled to a (single) bosonic heat bath [A7]. Again, the driving comes into play at two stages: First, it renormalizes the coherent dynamics and, second, the spectral density of the bath has to be evaluated at the energies of all sidebands. The latter corresponds to modifying the auto-correlation function of the bath operators, similar to the replacement (2.24).

In Ref. [A7], we studied a model whose static part of the Hamiltonian reads

$$H_0 = -\frac{\Delta}{2}\sigma_z + \sigma_x\,\xi, \tag{2.25}$$

where $\sigma_{x,z}$ denote Pauli spin matrices and ξ is a shorthand notation for quantum noise due to the bath operators. As a driving, the two possibilities $H_a = \sigma_x a\cos(\Omega t)$ and $H_b = \sigma_z b\cos(\Omega t)$ were considered. Since H_a commutes with the system-bath coupling, the transformation with U_0 renormalizes the system Hamiltonian while the coupling remains unaffected. The opposite is true for H_b: It keeps the system Hamiltonian unchanged, but modifies the coupling to the bath such that the bath correlation function now has to be evaluated also at the sideband energies. For appropriate parameters, both kinds of driving stabilize the coherence of the dissipative two-level system [A7]. Such effects have been observed in nuclear magnetic resonance [130–132] and, moreover, are discussed in the context of quantum information.

3 Transport through resonantly driven molecular wires

A natural starting point for the experimental investigation of molecular conduction under the influence of laser fields is the observation of resonant excitations of electrons from the donor and the acceptor site to bridge levels. As a working model we consider a so-called bridged molecular wire consisting of a donor and an acceptor site and $N-2$ sites in between (cf. Fig. 3.1). Each of the N sites is coupled to its nearest neighbors by a hopping matrix element Δ. The dipole force (1.8) of the laser field renders each level oscillating in time with a position-dependent amplitude. The energies of the donor and the acceptor orbitals, $|1\rangle$ and $|N\rangle$, are assumed to be close to the chemical potentials of the attached leads, $E_1 = E_N \approx \mu_L \approx \mu_R$. The bridge levels E_n, $n = 2, \ldots, N-1$, lie $E_B \gg \Delta, eV$ above the chemical potential.

Static conductor

Let us discuss first the static problem in the absence of the field, i.e., for $A = 0$. In the present case where the coupling energy between two neighboring sites is much smaller than the bridge energy, $\Delta \ll E_B$, one finds two types of eigenstates: One group of states is located on the bridge. It consists of $N-2$ levels with energies in the range $[E_B - 2\Delta, E_B + 2\Delta]$. In the absence of the driving field, these bridge states mediate the super-exchange between the donor and the acceptor. The two remaining states form a doublet whose states are approximately given by $(|1\rangle \pm |N\rangle)/\sqrt{2}$. Its splitting can be estimated in a perturbative approach [133] and is approximately given by $2\Delta(\Delta/E_B)^{N-2}$. Thus, the wire can be reduced to a two-level system with the effective tunnel matrix element $\Delta_{DA} = \Delta \exp[-\kappa(N-2)]$, where $\kappa = \ln(E_B/\Delta)$. If the chemical potentials of the leads are such that $\mu_L > E_D$ and $\mu_R < E_A$, i.e., for a voltage which is larger than the tunnel splitting but still much smaller than the bridge height, the current is dominated by the total transmission and for $\Gamma \gg \Delta_{DA}$ can be evaluated to read

$$I_0 = \frac{2e|\Delta|^2}{\Gamma} \mathrm{e}^{-2\kappa(N-2)}. \tag{3.1}$$

For the explicit calculation see, e.g. Ref. [A6]. In particular, one finds an exponentially decaying length dependence of the current [9,13]. Moreover, in this limit, it is also possible to evaluate explicitly the zero-frequency noise to obtain the Fano factor $F = \bar{S}/e|\bar{I}| = 1$. This value has a direct physical interpretation: Since the transmissions of electrons across a large barrier are rare and uncorrelated events, they obey Poisson statistics and, thus, variance and mean value are equal which translates to a Fano factor of one [88].

Resonant excitations

The magnitude of the current changes significantly when a driving field with a frequency $\Omega \approx E_B/\hbar$ is switched on. Then the resonant bridge levels merge with the donor and

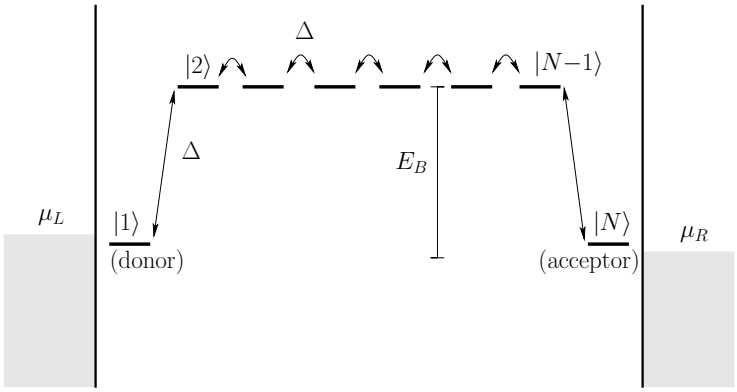

Figure 3.1: Bridged molecular wire consisting of $N = 8$ sites of which the terminating sites are coupled to leads with chemical potentials μ_L and $\mu_R = \mu_L - eV$.

the acceptor state to form a Floquet state. This opens a direct channel for the transport resulting in an enhancement of the electron current.

In order to estimate the magnitude of the current through the resonantly driven wire, we disregard all bridge levels besides the one that is in resonance with the donor and the acceptor. Let us assume that this resonant bridge level $|\psi_B\rangle$ extends over the whole bridge such that it comprises the sites $|2\rangle, \ldots, |N-1\rangle$ with equal probability amplitude $1/\sqrt{N-2}$. Accordingly, the overlap between the bridge level and the donor/acceptor becomes

$$\langle 1|H_{\text{molecule}}|\psi_B\rangle = \frac{\langle 1|H_{\text{molecule}}|2\rangle}{\sqrt{N-2}} = \frac{\Delta}{\sqrt{N-2}} = \langle \psi_B|H_{\text{molecule}}|N\rangle, \tag{3.2}$$

while the resonance condition defines the energy of the bridge level as

$$\langle \psi_B|H_{\text{molecule}}|\psi_B\rangle = \hbar\Omega. \tag{3.3}$$

It is now possible to apply an approximation scheme in the spirit of the high-frequency approximation described in Sec. 2.3; for details see Ref. [A8]. Thereby one derives for the *time-dependent* system the *static* effective Hamiltonian

$$H_{\text{molecule,eff}} = \begin{pmatrix} 0 & b & 0 \\ b & 0 & b \\ 0 & b & 0 \end{pmatrix}, \tag{3.4}$$

which describes a wire consisting of three levels with equal on-site energy and the tunnel matrix element renormalized according to

$$\Delta \longrightarrow b = \frac{J_1(A/\hbar\Omega)}{\sqrt{N-2}}\Delta, \tag{3.5}$$

where J_1 denotes the first-order Bessel function of the first kind.

The situation described by the Hamiltonian (3.4) is essentially the following: The central site $|\psi_B\rangle$ is coupled by matrix elements b to the donor and the acceptor site. Since

the latter couple to the external leads with a self energy $\Gamma/2$, their density of states is

$$\varrho(E) = \frac{1}{\pi}\frac{\Gamma/2}{E^2 + \Gamma^2/4}. \tag{3.6}$$

Then, the tunneling from and to the central site is determined by the golden rule rate

$$w = \frac{2\pi}{\hbar}|b|^2\varrho(0). \tag{3.7}$$

Like in the static case, we assume that the chemical potential of the left (right) lead lies above (below) the on-site energy of the donor (acceptor) and that therefore the donor is always occupied while the acceptor is always empty. Then, the electron tunneling rate from the central site to the acceptor is given by the golden rule rate (3.7) times the occupation probability p of the state $|\psi_B\rangle$. Accordingly, the rate of electrons from the donor to $|\psi_B\rangle$ is given by w times the probability $(1-p)$ to find the central site empty. Consequently, the occupation of the resonant bridge level evolves according to the master equation $\dot{p} = w(1-p) - wp$ with the stationary solution $p = 1/2$. Thus, for resonant excitations, the dc contribution of the time-dependent current is given by

$$\bar{I}_{\rm res} = e\,w\,p = e\frac{2A^2\Delta^2}{(N-2)\hbar^3\Omega^2\Gamma}. \tag{3.8}$$

Here, we have used the approximation $J_1(x) \approx x$ which is valid for small arguments of the Bessel function. As a major difference to the static case, the dc current (3.8) obeys an intriguing scaling behavior as a function of the wire length: Instead of the exponentially decaying length dependence (3.1) that has been found for the static case, in the presence of resonant driving, a scaling $\bar{I} \propto 1/N$ emerges. In particular for longer wires, this means that the external field enhances the conductance significantly.

Numerical results

In order to corroborate the analytical estimates presented above, we treat the transport problem defined by the wire Hamiltonian numerically by solving the corresponding Floquet equation (2.15) and a subsequent evaluation of the expressions (2.11) and (2.19) for the dc current and the zero-frequency noise, respectively. For a wire with $N = 5$ sites, one finds peaks in the current when the driving frequency matches the energy difference between the donor/acceptor doublet and one of the $N - 2 = 3$ bridge levels, cf. the solid line in Fig. 3.2a. The applied voltage is always chosen so small that the bridge levels lie well below the chemical potentials of the leads. In Figure 3.2a, the scale of the abscissa is chosen proportional to $(N-1)$ such that it suggests a common envelope function. Furthermore, we find from Fig. 3.2b that the dc current is proportional to A^2/Γ provided that A is sufficiently small and Γ sufficiently large. Thus, the numerical results indicate that the height of the current peaks obeys $\bar{I}_{\rm peak} \propto A^2/(N-1)\Gamma$ [A2], which is essentially in accordance with our analytical estimate (3.8). The main discrepancy comes from the fact that the overlap between the resonant level and the donor/acceptor differs from the estimate (3.2) by a numerical factor of the order one. Moreover, Fig. 3.2c demonstrates that, at the resonances, the Fano factor assumes values considerably lower than unity, $F \approx 1/2$, as in the case of resonant tunneling through a single level [30].

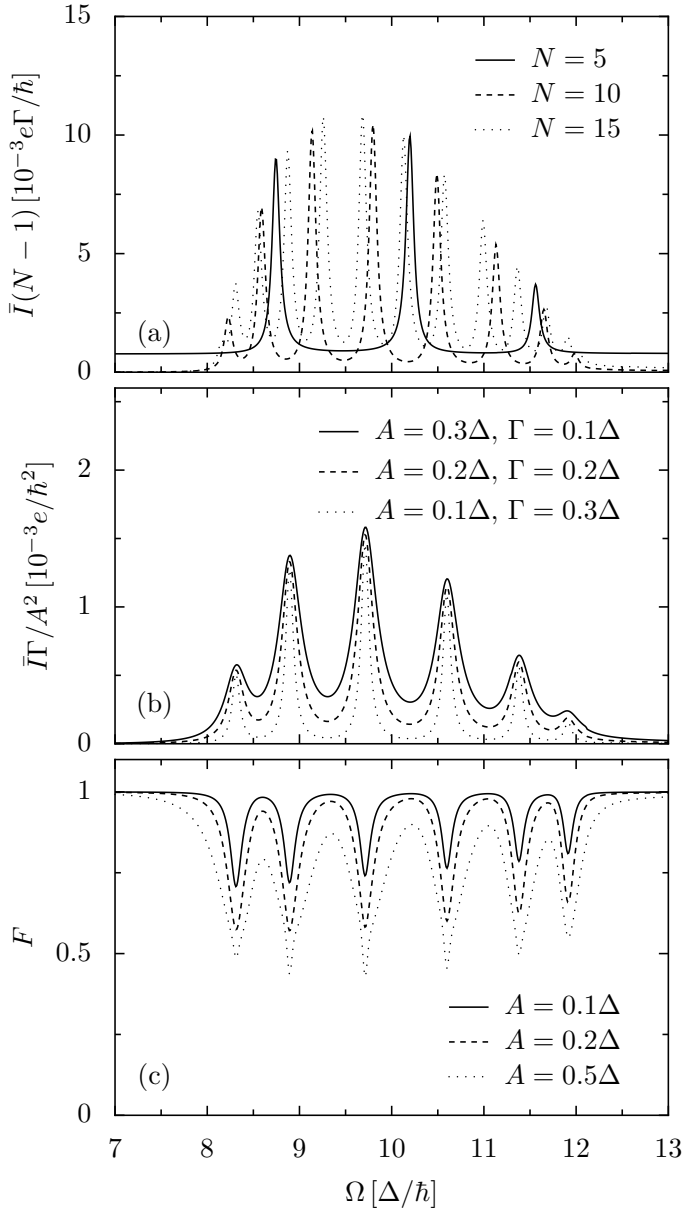

Figure 3.2: Exact numerical evaluation of the average current within Floquet formalism. (a) Average current $\bar{I}$ as a function of the the driving frequency Ω for various wire length N. The scaled amplitude is $A = 0.1\Delta$; the applied voltage $\mu_R - \mu_L = 5\Delta/e$. The other parameters read $\Gamma = 0.1\Delta$, $E_B = 10\Delta$, and $k_BT = 0$. (b) Average current for various driving amplitudes A and coupling strengths Γ for a wire of length $N = 8$. (c) Fano factor $F = \bar{S}/e\bar{I}$ for the wire length $N = 8$ and the wire-lead coupling $\Gamma = 0.1\Delta$. From Ref. [A8].

4 Non-adiabatic electron pumping

A widely studied phenomenon in driven transport is the so-termed ratchet effect: the conversion of ac forces without a net bias into directed motion [41–44, 134, 135]. The investigation of this phenomenon has been triggered by the question whether an asymmetric device can act as a Maxwell demon, i.e., whether it is possible to ultimately convert noise into work. Feynman's famous "ratchet and pawl" driven by random collisions with gas molecules, on first sight, indeed suggests that such a Maxwell demon exists. At thermal equilibrium, however, the whole nano-device obeys the same thermal fluctuations as the surrounding gas molecules. Therefore, consistent with the second law of thermodynamics, no directed motion occurs [136] and one has to conclude that the ratchet effect can be observed only in situations far from equilibrium.

A basic model, which captures the essential physics of ratchets, is an asymmetric, periodic potential under the influence of an ac driving. In such a system, even in the absence of any net bias, directed transport has been predicted for overdamped classical Brownian motion [41, 44] and also for dissipative quantum Brownian motion in the incoherent regime [45,46]. A related effect is found in the overdamped limit of dissipative tunneling in driven superlattices. There, the spatial symmetry is typically preserved and the directed transport is brought about by a driving field that includes higher harmonics of the driving frequency [137–139].

In the context of mesoscopic conduction, it has been found that the cyclic adiabatic change of the conductor parameters can induce a so-called pump current, where the charge pumped per cycle is determined by the area of parameter space enclosed during the cyclic evolution [20, 22, 140]. This relates the pump current to a Berry phase [21, 47]. Beyond the adiabatic regime, pump effects have been investigated theoretically [24, 37, 48, 56, 104] and also been measured in coupled quantum dots [16, 54, 141]. Since in the non-adiabatic regime, the main contribution to the pump current comes from electrons considerably below the Fermi surface, non-adiabatic electron pumping is essentially temperature independent [23].

The studies presented in this chapter were mainly motivated by two aspects: First, although infinitely extended "ideal" ratchets are convenient theoretical models, any experimental realization will have finite length, i.e., consist of a finite number of elementary units; cf. Fig. 4.2, below. Thus, finite size effects become relevant and it is intriguing to know the number of coupled wire units that are needed to mimic the behavior of a practically infinite system. Second, prior studies of quantum ratchets focussed on incoherent tunneling [45, 46]. By contrast, the present setup allows to investigate ratchet dynamics in the coherent quantum regime which has not been explored previously.

The results of this section, have originally [A1, A4] been computed for finite temperatures within the master equation approach of Sec. 2.1. In the limit of zero temperature, but otherwise equal parameters, the results from that perturbative treatment agree almost perfectly with the exact solution obtained from Eq. (2.11).

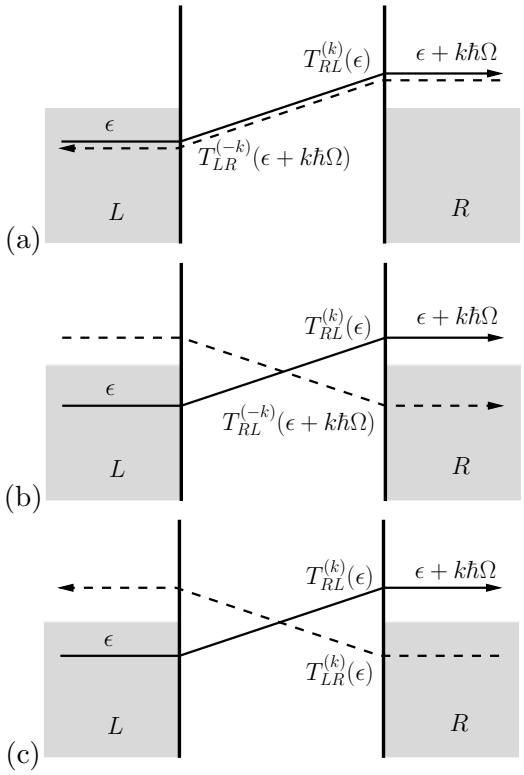

Figure 4.1: Scattering process of an electron with energy ϵ under the absorption of k photons (solid line) and its symmetry related partner (dashed) for time-reversal symmetry (a), time-reversal parity (b), and generalized parity (c). The processes depicted in each panel occur with equal probability.

Symmetry considerations

It is known from the study of deterministically rocked periodic potentials [142] and of driven classical Brownian particles [143] that the symmetry of the equations of motion may rule out any non-zero average current at asymptotic times. Thus, before starting to compute ratchet currents, let us first analyze what kind of symmetries may prevent the effect. We consider situations, where the electron distributions in both leads are identical—in particular, situations where both leads are in thermal equilibrium with a common chemical potential, $f_L(\epsilon) = f_R(\epsilon) \equiv f(\epsilon)$ for all ϵ. Then, no electromotive force acts and, consequently, in the absence of driving, all currents must vanish. An applied driving field, however, violates the equilibrium condition and can entail a finite dc current

$$I_{\text{pump}} = \frac{e}{h} \sum_k \int \mathrm{d}\epsilon \left[T_{LR}^{(k)}(\epsilon) - T_{RL}^{(k)}(\epsilon) \right] f(\epsilon). \tag{4.1}$$

Obviously, I_{pump} vanishes if the condition $T_{LR}^{(k)}(\epsilon) = T_{RL}^{(k)}(\epsilon)$ is fulfilled for all k and ϵ.

One might now ask whether this condition can be ensured by any symmetry relation. Relevant symmetries which come to mind are time-reversal symmetry, time-reversal parity,

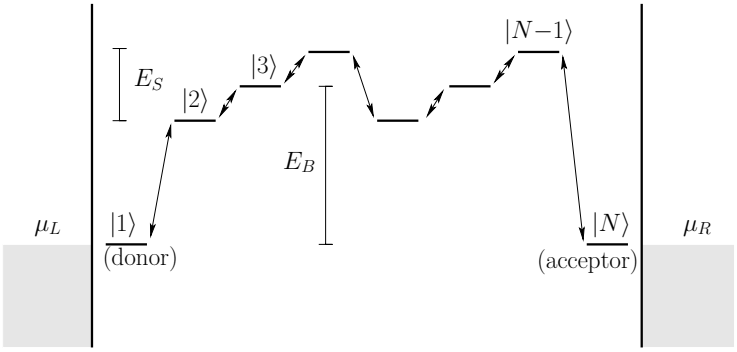

Figure 4.2: Level structure of the wire ratchet with $N = 8$ sites, i.e., $N_g = 2$ asymmetric molecular groups. The bridge levels are E_B above the donor and acceptor levels and are shifted by $\pm E_S/2$.

and generalized parity, which are defined by the operations

$$\mathcal{S}_{\mathrm{T}} \quad : t \to -t, \tag{4.2}$$

$$\mathcal{S}_{\mathrm{TP}} : (x,t) \to (-x,-t), \tag{4.3}$$

$$\mathcal{S}_{\mathrm{GP}} : (x,t) \to (-x,t+\mathcal{T}/2), \tag{4.4}$$

respectively. Note that time-reversal, in addition to $t \to -t$, requires to replace the transition amplitude $G(t,t')$ by its complex conjugate [144]. From the definition of $G^{(k)}(\epsilon)$, see Eq. (2.12), follows that, provided the wire-lead Hamiltonian (1.1) obeys the corresponding symmetry, the transmissions in each panel of Fig. 4.1 occur with equal probability. Obviously, only the generalized parity $\mathcal{S}_{\mathrm{GP}}$ directly yields $T^k_{LR}(\epsilon) = T^k_{RL}(\epsilon)$ such that the average current (4.1) vanishes. By contrast, the presence of time-reversal symmetry still allows a finite I_{pump}. Time-reversal parity $\mathcal{S}_{\mathrm{TP}}$ has some rather subtle consequence [A4]: Expanding the transmission in powers of the wire-lead coupling Γ, one finds that under this symmetry, the current vanishes to linear order. This means that for a ratchet with time-reversal parity, we no longer find the generic behavior $I_{\mathrm{pump}} \propto \Gamma$, but rather $I_{\mathrm{pump}} \propto \Gamma^2$.

In the following, we consider two typical cases where generalized parity is broken and, thus, a pump current emerges, namely (i) an asymmetric structure under the influence of a harmonic dipole force, the so-called rocking ratchet, and (ii) a spatially symmetric system for which generalized parity is broken dynamically by mixing with higher harmonics.

Spatial symmetry breaking: coherent quantum ratchets

A straightforward way to break generalized parity, is the use of a conductor with an asymmetric level structure. Then, already a purely harmonic dipole driving $a(t) = A\sin(\Omega t)$ in the Hamiltonian (1.8) is sufficient to generate a dc current. As a tight-binding model of such a structure, we have considered a wire consisting of a donor and an acceptor site and N_g asymmetric groups in the ratchet-like configuration sketched in Fig. 4.2. In molecular structures, such an asymmetry can be achieved in many ways, and was explored as a source of molecular rectifying since the early work of Aviram and Ratner [145] and later found

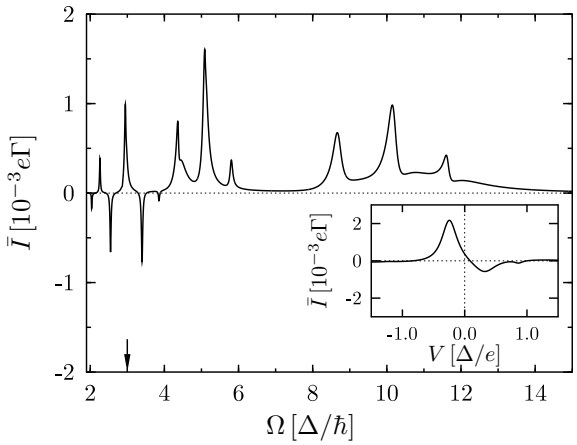

Figure 4.3: Time-averaged current as a function of the driving frequency Ω for $A = 2\Delta$ and $N_g = 1$. The bridge parameters are $E_B = 10\Delta$, $E_S = \Delta$, the driving frequency is $\Omega = 3\Delta/\hbar$, the coupling to the leads is chosen as $\Gamma_L = \Gamma_R = 0.1\Delta/\hbar$, and no voltage is applied, $\mu_L = \mu_R$. The temperature is $k_BT = 0.25\Delta$. The inset displays the dependence of the average current on an externally applied static voltage V, which we assume here to drop linearly along the molecule. The driving frequency is $\Omega = 3\Delta/\hbar$ (cf. arrow in main panel). From Ref. [A1].

experimentally [3, 63]. In general, it can be controlled by attaching different chemical groups to the opposite sides of an otherwise symmetric molecular wire [3, 63, 146]. In our model, the inner wire states are arranged in N_g groups of three, i.e. $N - 2 = 3N_g$. In each group, the first (last) level is lowered (raised) by an energy $E_S/2$, forming an asymmetric saw-tooth like structure. The energies of the donor and the acceptor orbitals are assumed to be at the level of the chemical potentials of the attached leads and since no voltage is applied, $E_1 = E_N = \mu_L = \mu_R$. The bridge levels E_n lie at E_B and $E_B \pm E_S/2$.

A quantitative analysis of a tight-binding model has demonstrated that the resulting ratchet currents lie in the range of 10^{-9}–10^{-8} A [A1] and, thus, can be measured with today's techniques. In the limit of very weak driving, we find $I_{\rm pump} \propto E_S A^2$ [A4]. This behavior is expected from symmetry considerations: On one hand, the asymptotic current must be independent of any initial phase of the driving field and therefore is an even function of the field amplitude A. On the other hand, $I_{\rm pump}$ vanishes for zero step size since then generalized parity is restored. This also indicates that the ratchet effect can only be obtained from a treatment beyond linear response.

While for rather short wires ($N_g \lesssim 3$), even the sign of the current may depend on the number N_g of asymmetric groups, the current becomes practically length-independent for wires that comprise five or more wire units [A1, A4]. As a practical consequence, already relatively short wires can mimic the behavior of an (infinitely extended) quantum ratchet. Moreover, the fact that $I_{\rm pump}$ converges to a finite value if the number of wire units is enlarged, demonstrates that the dissipation caused by the coupling to the leads is sufficient to establish the ratchet effect in the limit of long wires. Figure 4.3 depicts the average current vs. the driving frequency Ω, exhibiting resonance peaks as a striking feature. Comparison with the quasienergy spectrum reveals that each peak corresponds to a non-

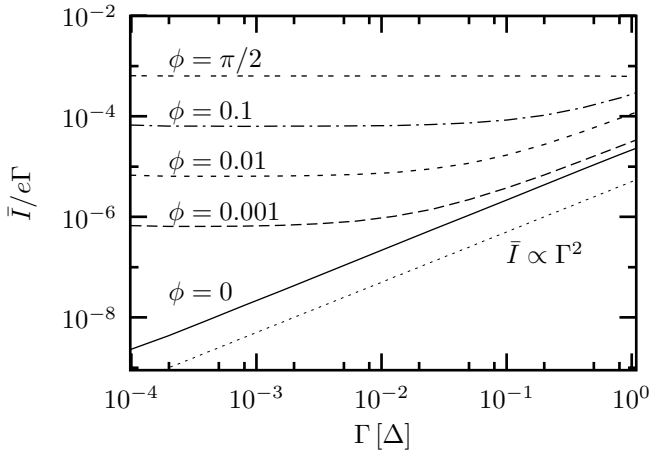

Figure 4.4: Average current response to the harmonic mixing signal with amplitudes $A_1 = 2A_2 = \Delta$, as a function of the coupling strength for different phase shifts ϕ. The remaining parameters are $\Omega = 10\Delta/\hbar$, $E_\mathrm{B} = 5\Delta$, $k_BT = 0.25\Delta$, $N = 10$. The dotted line is proportional to Γ; it represents a current which is proportional to Γ^2. From Ref. [A4].

linear resonance between the donor/acceptor and a bridge orbital. While the broader peaks at $\hbar\Omega \approx E_B = 10\Delta$ match the 1:1 resonance (i.e. the driving frequency equals the energy difference), one can identify the sharp peaks for $\hbar\Omega \lesssim 7\Delta$ as multi-photon transitions. The appearance of these resonance peaks clearly demonstrates that the conductor in Fig. 4.2 acts as a *coherent* quantum ratchet. As a consequence of the broken spatial symmetry of the wire, one expects an asymmetric current-voltage characteristic. This is indeed found as depicted in the inset of Fig. 4.3.

Moreover, the ratchet current possesses accidental zeros, i.e., it vanishes at isolated points of parameter space although symmetry permits a non-zero value [A1]. Such parameter values are particularly interesting for applications since there, by variation of one parameter the current can be routed towards the one or the other direction.

Dynamical symmetry breaking: harmonic mixing

A pump effect is also found for spatially symmetric wires with the level structure sketched in Fig. 3.1. Then, the static part of the wire Hamiltonian (1.8) obeys parity symmetry and, thus, for purely harmonic driving, generalized parity rules out a non-zero dc current. In order to break generalized parity in a dynamical way, we add a second harmonic, i.e., a contribution with twice the fundamental frequency, to the driving field. Thus, we consider

$$a(t) = A_1 \sin(\Omega t) + A_2 \sin(2\Omega t + \phi). \tag{4.5}$$

While now shifting the time t by half a driving period, i.e. by π/Ω, changes the sign of the fundamental frequency contribution, the second harmonic is left unchanged. The generalized parity is therefore no longer present and we expect to find a non-vanishing average current.

The phase shift ϕ here plays a subtle role. For $\phi = 0$ (or equivalently any multiple of π) the dipole Hamiltonian (1.8) is invariant under the time-reversal parity (4.3). Therefore,

as argued above, the pump current vanishes to linear order in the wire-lead coupling Γ [A4]. Since the higher-order contributions typically remain finite, one expects a dc current $I_{\mathrm{pump}} \propto \Gamma^2$. Figure 4.4 confirms this prediction. Yet one observes that already a small deviation from $\phi = 0$ is sufficient to restore the usual weak coupling behavior, namely a current which is proportional to the coupling strength Γ. For very weak coupling and small driving amplitudes, we find a pump current proportional to $\sin\phi$; with increasing wire-lead coupling, the phase dependence of the current shifts towards $\cos\phi$ [A10]. As a potential application, this effect bears the possibility of sensitively detecting phase lags between the fundamental mode and the second harmonic.

Other features of the harmonic mixing current resemble the ones discussed in the preceding section for ratchet-like wires. In particular, we again find current reversals and also that the current becomes essentially independent of the wire length. Typically, the current reaches convergence for a length $N \gtrsim 10$ [A4].

Phonon damping

Including also the coupling of the wire electrons to a phononic heat bath, one can no longer employ the scattering formula (2.11) and, thus, has to resort to the master equation approach of Sec. 2.1 for the computation of the dc current. Here we only mention the main findings and refer the reader to the original work, Ref. [A10]: The presence of phonon damping, generally increases the pump current up to one order of magnitude. This means that for quantum ratchets, noise plays a rather constructive role. Moreover, phonon damping influences the dependence of the current on the phase lag since it provides an additional shift towards a $\cos\phi$ behavior.

5 Coherent current control

A prominent example for the control of quantum dynamics is the so-called coherent destruction of tunneling, i.e., the suppression of the tunneling dynamics of a particle in a double-well potential [49] and in a two-level system [49, 50]. Recently, coherent destruction of tunneling has also been found for the dynamics of two interacting electrons in a double quantum dot [52, 129]. A closely related phenomenon is the miniband collapse in ac-driven superlattices which yields a suppression of quantum diffusion [51, 107, 147]. In this chapter, we address the question whether a corresponding transport effect exists: If two leads are attached to the ends of a driven tunneling system, is the suppression of tunneling visible in conductance properties? Since time-dependent control schemes can be valuable in practice only if they operate at tolerable noise levels, the question is also whether the corresponding noise strength can be kept small or even be controlled.

Coherent destruction of tunneling

In order to introduce the reader to the essentials of coherent destruction of tunneling in isolated quantum systems, we consider a single particle in a driven two-level system described by the Hamiltonian

$$H_{\mathrm{TLS}}(t) = -\frac{\Delta}{2}\sigma_x + \frac{A}{2}\sigma_z \cos(\Omega t). \tag{5.1}$$

If the energy of the quanta $\hbar\Omega$ of the driving field exceeds the energy scales of the wire, one can apply the high-frequency approximation scheme of Sec. 2.3 [A6, 50] and finds that the dynamics can be described approximately by the static effective Hamiltonian (2.22) which in the present case becomes

$$\bar{H}_{\mathrm{TLS,eff}} = -\frac{\Delta_{\mathrm{eff}}}{2}\sigma_x, \tag{5.2}$$

with the tunnel matrix element renormalized according to

$$\Delta \longrightarrow \Delta_{\mathrm{eff}} = J_0(A/\hbar\Omega)\Delta. \tag{5.3}$$

Again, J_0 denotes the zeroth order Bessel function of the first kind. If the ratio $A/\hbar\Omega$ equals a zero of the Bessel function J_0 (i.e., for the values 2.405.., 5.520.., 8.654.., ...), the effective tunnel matrix vanishes and the tunneling is brought to a standstill.

This reasoning is readily generalized to other tight-binding systems: If neighboring sites are coupled by a hopping matrix element Δ and the difference of their on-site energies oscillates with an amplitude A, one finds that the physics is determined by the renormalized matrix element (5.3), provided that $\hbar\Omega$ is the largest energy scale.

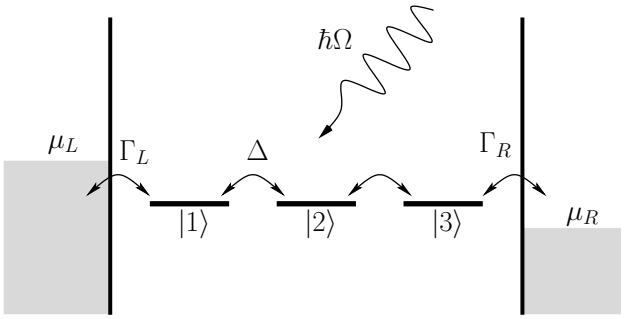

Figure 5.1: Level structure of the molecular wire with $N = 3$ orbitals. The end sites are coupled to two leads with chemical potentials μ_L and $\mu_R = \mu_L - eV$.

Current and noise suppressions

In order to investigate coherent destruction of tunneling in the context of transport, we consider the wire-lead setup sketched in Fig. 5.1 where the wire is described by the dipole Hamiltonian (1.8) with on-site energies $E_n = 0$. The wire is assumed to couple equally to both leads, $\Gamma_L = \Gamma_R = \Gamma$, and the numerical results are computed with the Floquet scattering approach of Sec. 2.2.

Figure 5.2a depicts the dc current and the zero-frequency noise for a wire with $N = 3$ sites and a relatively large applied voltage, $\mu_L - \mu_R = 50\Delta$. As a remarkable feature, we find that for certain values of the field amplitude A, the current drops to a value of some percent of the current in the absence of the field [A3, A5] with a suppression factor which is fairly independent of the wire-lead coupling Γ [A10]. The corresponding noise strength $\bar{S}$ exhibits similar suppressions and, in addition, has some small plateaus in the vicinity of the minima. The role of the plateaus is elucidated by the *relative* noise strength characterized by the Fano factor (1.18) which is shown in Fig. 5.2b. Interestingly enough, we find that the Fano factor as a function of the driving amplitude A possesses both a sharp maximum at each current suppression and two pronounced minima nearby. For a sufficiently large voltage, the Fano factor at the maximum assumes the value $F \approx 1/2$. Once the driving amplitude is of the order of the applied voltage, however, the Fano factor becomes much larger. The relative noise minima are distinct and provide a typical Fano factor of $F \approx 0.15$. Reducing the coupling to the leads renders these phenomena even more pronounced since then the suppressions occur in a smaller interval of the driving amplitude, cf. Fig. 5.2b. The overall behavior is robust in the sense that approximately the same values for the minima and the maximum are also found for larger wires, different driving frequencies, different coupling strengths, and slightly modified on-site energies, provided that $\Delta, \Gamma, E_n \ll \hbar\Omega$ and that the applied voltage is sufficiently large [A9].

The behavior of the current and the noise can be understood within the high-frequency approximation discussed in Sec. 2.3 where, one replaces the tunneling matrix element Δ and the Fermi functions $f_{L,R}(\epsilon)$ by the corresponding effective quantities, cf. Eqs. (2.23) and (2.24). Then, current and noise are computed from the static expressions (1.14) and (1.17), respectively. In the limit of very large voltages, $eV \gtrsim A$ we employ the relation $J_k(x) \approx 0$ for $k > x$ [148] and find that the effective electron distributions in

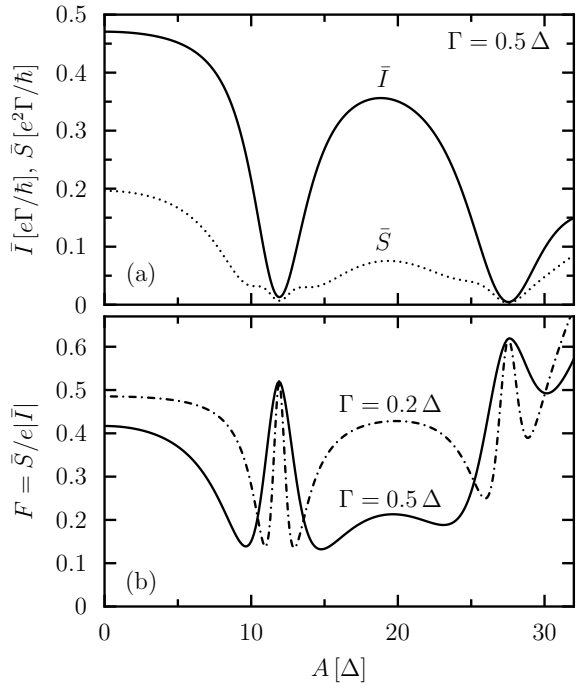

Figure 5.2: Time-averaged current $\bar{I}$ and zero-frequency noise $\bar{S}$ (a) as a function of the driving amplitude A for a wire with $N = 3$ sites with on-site energies $E_n = 0$ and chemical potentials $\mu_R = -\mu_L = 25\Delta$. The other parameters read $\Omega = 5\Delta/\hbar$, $\Gamma = 0.5\Delta$, and $k_BT = 0$. Panel (b) displays the Fano F factor for these parameters (full line) and for smaller wire-lead coupling (dash-dotted line). From Ref. [A5].

the left and the right lead, in the relevant energy range, become practically one or zero, respectively. As a consequence, the current and the noise are determined by the total transmission which is proportional to $|\Delta_{\rm eff}|^2$. In particular, the transmission vanishes if the condition $J_0(A/\hbar\Omega) = 0$ is fulfilled. The behavior of the Fano factor is determined by the crossover from $|\Delta_{\rm eff}| \gg \Gamma$ to $|\Delta_{\rm eff}| \ll \Gamma$. Both limits correspond to the transport through a symmetric double barrier with either the wire-lead coupling or the intra-wire coupling being the bottleneck. Thus, both limits are characterized by $F \approx 1/2$ [30]. At the crossover $|\Delta_{\rm eff}| \approx \Gamma$ the effective barriers vanish and, consequently, the Fano factor assumes its minimum. Note that the quenching of transmission observed in Ref. [149,150] does not result from a renormalized inter-well tunnel matrix element, but rather originates from the appearance of the Bessel function J_0 in the effective electron distribution (2.24).

For lower voltages, $eV \lesssim A$, the effective electron distributions can no longer be approximated by zero or one. The modification can be captured by a correction factor which is given by a sum over squares of Bessel functions [A6, A9]. Still the comparison between the high-frequency approximation and the exact solution shows excellent agreement, as has been demonstrated explicitly for the transport through a driven two-level system [A6].

For a much lower driving frequency of the order of the wire excitations, $\Omega = \Delta/\hbar$, the high-frequency approximation is no longer applicable. Nevertheless, the average current exhibits clear minima with a suppression factor of the order of 1/2. Compared to the

high-frequency case, these minima are shifted towards smaller driving amplitudes, i.e., they occur for ratios $A/\hbar\Omega$ slightly below the zeros of the Bessel function J_0. At the minima of the current, the Fano factor still assumes a maximum with a value close to $F \approx 1/2$. Although the sharp minima close to the current suppressions have vanished, in-between the maxima the Fano factor assumes remarkably low values of $F \approx 0.2$; cf. Fig. 3 of Ref. [A9].

In a realistic experimental setup, the on-site energies of the wire might be distorted by the applied transport voltage which rearranges the charge distribution in the conductor and thereby causes an internal potential profile [151–153]. For quantum dots, this influence can be counterbalanced by gate voltages. Still, it is desirable to investigate the influence of an internal bias. Surprisingly, the behavior of the average current is fairly stable even against a large bias. In particular, we still find pronounced current suppressions [A3, A9]. By contrast, the minima of the Fano factor fade out: Once the energy difference between two neighboring sites becomes of the order of the wire-lead coupling, the structure in the Fano factor vanishes and one finds $F \approx 1/2$, unless the driving amplitude is so large that finite-voltage effects start to play a role; cf. Fig. 5 of Ref. [A9].

Phonon damping

A further question to be addressed is the robustness of the current suppressions against dissipation. In the corresponding tunneling problem, the driving alters both the coherent and the dissipative time scale by the same factor [A7]. Thus, one might speculate that a vibrational coupling leaves the effect of the driving on the current qualitatively unchanged. This, however, is not the case: With increasing dissipation strength, the characteristic current suppressions become washed out until they finally disappear when the damping strength becomes of the order of the tunnel coupling Δ [A10]. This detracting influence underlines the importance of quantum coherence for the observation of those current suppressions. Moreover, for the model employed in Ref. [A10], we do not find the analogue of the effect of a stabilization of coherent destruction of tunneling within a certain temperature range [154–156] or, likewise, with increasing external noise [157], as it has been reported for driven, dissipative symmetric bistable systems.

6 Summary and outlook

We have studied various aspects of the electron transport through time-dependent tight-binding systems. For the theoretical description, two formalisms have been employed which both take advantage of the Floquet theorem. A Floquet scattering approach provides an exact solution of the time-dependent transport problem and, moreover, yields an expression for the noise power. Interestingly, unlike in the time-independent case, the noise depends also on the phases of the transmission amplitudes. As a drawback, this approach is limited to the case of purely coherent transport in the absence of electron-electron interactions. As soon as other degrees of freedom like, e.g. a phonon bath, come into play, it is advantageous to resort to other formalisms like a Floquet master equation approach which, however, is perturbative in the wire-lead coupling.

Of foremost interest in view of ongoing experiments, is the enhancement of molecular conduction by resonant excitations. We have derived an analytical expression for the current enhancement factor and, moreover, have found that the shot noise is reduced approximately by a factor of one half.

Both molecular wires and quantum dot arrays can act as coherent quantum ratchets and thereby operate in a regime where ratchet dynamics has not been studied previously. Of particular practical relevance is the fact that already relatively short wires or arrays behave like infinite systems. A symmetry analysis revealed that a ratchet or pump effect in a wire-lead setting can only be observed in the absence of generalized parity. This leads to the idea of pumping in a entirely symmetric system by harmonic mixing.

Coherent destruction of tunneling has a corresponding transport effect which exhibits an even richer variety of phenomena. For driving parameters where the tunneling in isolated unbiased systems is suppressed, the dc current drops to a small residual value. This effect is found to be stable against a static bias. Moreover, investigation of the corresponding noise level characterized by the Fano factor, has revealed that the current suppressions are accompanied by a noise maximum and two remarkably low minima. This allows to selectively control both the current and its noise by ac fields.

Many more intriguing phenomena await being unraveled or are at present under study. Of interest for potential applications are the noise properties of non-adiabatic pumps. For resonant excitations, these can be treated analytically within an approximation scheme in the spirit of the one applied in Ref. [A6]. Moreover, there is experimental evidence that the coupling of the electrons to single vibrational modes of the molecule is relevant for molecular conductance. Thus, the wire-lead model should be extended by single phonon modes. Even in the absence of driving, the influence of an applied voltage to the asymptotic state of such a single phonon mode is still an unanswered question.

Acknowledgements

First, I would like to express my gratitude to Peter Hänggi and Gert-Ludwig Ingold for their continued support and their interest in my research during the last years. Their ideas were of great influence on this work.

For the fruitful collaboration during the course of this work, I like to thank Sébastien Camalet, Karen M. Fonseca Romero, Abraham Nitzan, Michael Straß, and, in particular, Jörg Lehmann who has been involved in the "wire project" from the very beginning.

During the recent years, I enjoyed many interesting and helpful discussions on molecular conduction and quantum dots with numerous colleagues. In particular, I have benefitted from discussions with U. Beierlein, G. Cuniberti, T. Dittrich, F. Grossmann, V. May, M. Rey, K. Richter, F. Sols, H. B. Weber, and J. Würfel.

References

[1] M. A. Reed, C. Zhou, C. J. Muller, T. P. Burgin, and J. M. Tour, Science **278**, 252 (1997).

[2] X. D. Cui, A. Primak, X. Zarate, J. Tomfohr, O. F. Sankey, A. L. Moore, T. A. Moore, D. Gust, G. Harris, and S. M. Lindsay, Science **294**, 571 (2001).

[3] J. Reichert, R. Ochs, D. Beckmann, H. B. Weber, M. Mayor, and H. von Löhneysen, Phys. Rev. Lett. **88**, 176804 (2002).

[4] P. Hänggi, M. Ratner, and S. Yaliraki (Eds.), *Processes in Molecular Wires*, Chem. Phys. **281**, 111 (2002).

[5] A. Nitzan and M. A. Ratner, Science **300**, 1384 (2003).

[6] J. R. Heath and M. A. Ratner, Physics Today **56**, 43 (2003).

[7] M. Di Ventra and N. D. Lang, Phys. Rev. B **65**, 045402 (2002).

[8] J. Heurich, J. C. Cuevas, W. Wenzel, and G. Schön, Phys. Rev. Lett. **88**, 256803 (2002).

[9] V. Mujica, M. Kemp, and M. A. Ratner, J. Chem. Phys. **101**, 6849 (1994).

[10] D. Segal, A. Nitzan, W. B. Davis, M. R. Wasielewski, and M. A. Ratner, J. Phys. Chem. **104**, 3817 (2000).

[11] D. Boese and H. Schoeller, Europhys. Lett. **54**, 668 (2001).

[12] E. G. Petrov and P. Hänggi, Phys. Rev. Lett. **86**, 2862 (2001).

[13] A. Nitzan, Annu. Rev. Phys. Chem. **52**, 681 (2001).

[14] M. H. Hettler, W. Wenzel, M. R. Wegewijs, and H. Schoeller, Phys. Rev. Lett. **90**, 076805 (2003).

[15] R. H. Blick, R. J. Haug, J. Weis, D. Pfannkuche, K. von Klitzing, and K. Eberl, Phys. Rev. B **53**, 7899 (1996).

[16] W. G. van der Wiel, S. De Francesoni, J. M. Elzerman, T. Fujisawa, S. Tarucha, and L. P. Kouwenhoven, Rev. Mod. Phys. **75**, 1 (2003).

[17] T. Fujisawa and S. Tarucha, Superlatt. Microstruct. **21**, 247 (1997).

[18] T. H. Oosterkamp, T. Fujisawa, W. G. van der Wiel, K. Ishibashi, R. V. Hijman, S. Tarucha, and L. P. Kouwenhoven, Nature **395**, 873 (1998).

[19] G. Platero and R. Aguado, Phys. Rep. **395**, 1 (2004).

[20] D. J. Thouless, Phys. Rev. B **27**, 6083 (1983).

[21] B. L. Altshuler and L. I. Glazman, Science **283**, 1864 (1999).

[22] M. Switkes, C. M. Marcus, K. Campman, and A. C. Gossard, Science **283**, 1905 (1999).

[23] M. Wagner and F. Sols, Phys. Rev. Lett. **83**, 4377 (1999).

[24] Y. Levinson, O. Entin-Wohlman, and P. Wölfle, Phys. Rev. Lett **85**, 634 (2000).

[25] R. Landauer, IBM J. Res. Dev. **1**, 223 (1957).

[26] Y. Imry, *Introduction to Mesoscopic Physics*, Vol. 1 of *Mesoscopic Physics and Nanotechnology* (Oxford University Press, New York, 1986).

[27] S. Datta, *Electronic Transport in Mesoscopic Systems* (Cambridge University Press, Cambridge, 1995).

[28] R. Landauer, Phys. Scr. **T42**, 110 (1992).

[29] Y. Imry and R. Landauer, Rev. Mod. Phys. **71**, S306 (1999).

[30] Ya. M. Blanter and M. Büttiker, Phys. Rep. **336**, 1 (2000).

[31] M. Henseler, T. Dittrich, and K. Richter, Europhys. Lett. **49**, 289 (2000).

[32] M. Henseler, T. Dittrich, and K. Richter, Phys. Rev. E **64**, 046218 (2001).

[33] W. Li and L. E. Reichl, Phys. Rev. B **60**, 15732 (1999).

[34] S. Datta and M. P. Anantram, Phys. Rev. B **45**, 13761 (1992).

[35] M. Wagner, Phys. Rev. Lett. **85**, 174 (2000).

[36] A.-P. Jauho, N. S. Wingreen, and Y. Meir, Phys. Rev. B **50**, 5528 (1994).

[37] C. A. Stafford and N. S. Wingreen, Phys. Rev. Lett. **76**, 1916 (1996).

[38] A. Prêtre, H. Thomas, and M. Büttiker, Phys. Rev. B **54**, 8130 (1996).

[39] M. H. Pedersen and M. Büttiker, Phys. Rev. B **58**, 12993 (1998).

[40] G. B. Lesovik and L. S. Levitov, Phys. Rev. Lett. **72**, 538 (1994).

[41] P. Hänggi and R. Bartussek, in *Nonlinear Physics of Complex Systems—Current Status and Future Trends*, Vol. 476 of *Lecture Notes in Physics*, edited by J. Parisi, S. C. Müller, and W. W. Zimmermann (Springer, Berlin, 1996), pp. 294–308.

[42] R. D. Astumian, Science **276**, 917 (1997).

[43] F. Jülicher, A. Adjari, and J. Prost, Rev. Mod. Phys. **69**, 1269 (1997).

[44] P. Reimann, Phys. Rep. **361**, 57 (2002).

[45] P. Reimann, M. Grifoni, and P. Hänggi, Phys. Rev. Lett. **79**, 10 (1997).

[46] M. Grifoni, M. S. Ferrreira, J. Peguiron, and J. B. Mejer, Phys. Rev. Lett. **89**, 146801 (2002).

[47] P. W. Brouwer, Phys. Rev. B **58**, 10135 (1998).

[48] B. Wang, J. Wang, and H. Guo, Phys. Rev. B **65**, 073306 (2002).

[49] F. Grossmann, T. Dittrich, P. Jung, and P. Hänggi, Phys. Rev. Lett. **67**, 516 (1991).

[50] F. Großmann and P. Hänggi, Europhys. Lett. **18**, 571 (1992).

[51] M. Holthaus, Phys. Rev. Lett. **69**, 351 (1992).

[52] C. E. Creffield and G. Platero, Phys. Rev. B **65**, 113304 (2002).

[53] A. H. Dayem and R. J. Martin, Phys. Rev. Lett. **8**, 246 (1962).

[54] W. G. van der Wiel, T. Fujisawa, T. H. Oosterkamp, and L. P. Kouwenhoven, Physica B **272**, 31 (1999).

[55] T. H. Stoof and Yu. V. Nazarov, Phys. Rev. B **53**, 1050 (1996).

[56] P. Brune, C. Bruder, and H. Schoeller, Phys. Rev. B **56**, 4730 (1997).

[57] D. Loss and D. P. DiVincenzo, Phys. Rev. A **57**, 120 (1998).

[58] J. M. Elzerman, R. Hanson, J. S. Greidanus, L. H. W. van Beveren, S. De Franceschi, L. M. K. Vandersypen, S. Tarucha, and L. P. Kouwenhoven, Phys. Rev. B **67**, 161308 (2003).

[59] T. Hayashi, T. Fujisawa, H. D. Cheong, Y. H. Jeong, and Y. Hirayama, Phys. Rev. Lett. **91**, 226804 (2003).

[60] A. Zrenner, E. Beham, S. Stufler, F. Findeis, M. Bichler, and G. Abstreiter, Nature **418**, 612 (2002).

[61] I. I. Rabi, Phys. Rev. **51**, 652 (1937).

[62] C. Kergueris, J.-P. Bourgoin, S. Palacin, D. Esteve, C. Urbina, M. Mgoga, and C. Joachim, Phys. Rev. B **59**, 12505 (1999).

[63] H. B. Weber, J. Reichert, F. Weigend, R. Ochs, D. Beckmann, M. Mayor, R. Ahlrichs, and H. von Löhneysen, Chem. Phys. **281**, 113 (2002).

[64] S. Datta, W. Tian, S. Hong, R. Reifenberger, J. I. Henderson, and C. P. Kubiak, Phys. Rev. Lett **79**, 2530 (1997).

[65] J. Würfel and H. B. Weber, private communication.

[66] D. M. Newns, Phys. Rev. **178**, 1123 (1969).

[67] V. Mujica, M. Kemp, A. Roitberg, and M. A. Ratner, J. chem. Phys. **104**, 7296 (1996).

[68] L. E. Hall, J. R. Reimers, N. S. Hush, and K. Silverbrook, J. Chem. Phys. **112**, 1510 (2000).

[69] F. Demming, J. Jersch, K. Dickmann, and P. I. Geshev, Appl. Phys. B **66**, 593 (1998).

[70] A. Otto, Phys. Stat. Sol. (a) **188**, 1455 (2001).

[71] M. Fleischmann, P. J. Hendra, and A. J. McQuillan, Chem. Phys. Lett. **26**, 163 (1974).

[72] D. L. Jeanmaire and R. P. V. Duyne, J. Electroanal. Chem. **84**, 1 (1977).

[73] B. Pellegrini, Il Nuovo Cimento **15**, 855 (1993).

[74] P. K. Tien and J. P. Gordon, Phys. Rev. **129**, 647 (1963).

[75] N. S. Wingreen, Appl. Phys. Lett. **56**, 253 (1990).

[76] V. Kislov and A. Kamenev, Appl. Phys. Lett. **59**, 1500 (1991).

[77] R. Aguado, J. Iñarrea, and G. Platero, Phys. Rev. B **53**, 10030 (1996).

[78] E. N. Economou and C. M. Soukoulis, Phys. Rev. Lett. **46**, 618 (1981).

[79] D. C. Langreth and E. Abrahams, Phys. Rev. B **24**, 2978 (1981).

[80] A. D. Stone and A. Szafer, IBM J. Res. Develop. **32**, 384 (1988).

[81] H.-L. Engquist and P. W. Anderson, Phys. Rev. B **24**, 1151 (1981).

[82] M. Büttiker, Phys. Rev. Lett. **57**, 1761 (1986).

[83] D. S. Fisher and P. A. Lee, Phys. Rev. B **23**, 6851 (1981).

[84] F. Sols, Phys. Rev. Lett. **67**, 2874 (1991).

[85] C. Caroli, R. Combescot, P. Noziere, and D. Saint-James, J. Phys. C **4**, 916 (1971).

[86] Y. Meir and N. S. Wingreen, Phys. Rev. Lett. **68**, 2512 (1992).

[87] N. S. Wingreen, A.-P. Jauho, and Y. Meir, Phys. Rev. B **48**, 8487 (1993).

[88] U. Fano, Phys. Rev. **72**, 26 (1947).

[89] S. Nakajima, Prog. Theor. Phys. **20**, 948 (1958).

[90] R. Zwanzig, J. Chem. Phys. **33**, 1338 (1960).

[91] T. Novotný, Europhys. Lett. **59**, 648 (2002).

[92] V. May and O. Kühn, *Charge and Energy Transfer Dynamics in Molecular Systems*, 2nd ed. (Wiley-VCH, Weinheim, 2003).

[93] P. Hänggi and H. Thomas, Phys. Rep. **88**, 206 (1982).

[94] C. Bruder and H. Schoeller, Phys. Rev. Lett. **72**, 1076 (1994).

[95] G. Floquet, Ann. de l'Ecole Norm. Sup. **12**, 47 (1883).

[96] J. H. Shirley, Phys. Rev. **138**, B979 (1965).

[97] H. Sambe, Phys. Rev. A **7**, 2203 (1973).

[98] N. L. Manakov, V. D. Ovsiannikov, and L. P. Rapoport, Phys. Rep. **141**, 319 (1986).

[99] R. Blümel, R. Graham, L. Sirko, U. Smilansky, H. Walther, and K. Yamada, Phys. Rev. Lett. **62**, 341 (1989).

[100] S. Kohler, T. Dittrich, and P. Hänggi, Phys. Rev. E **55**, 300 (1997).

[101] M. Grifoni and P. Hänggi, Phys. Rep. **304**, 229 (1998).

[102] A. Buchleitner, D. Delande, and J. Zakrzewski, Phys. Rep. **368**, 409 (2002).

[103] P. Jung, Phys. Rep. **234**, 175 (1993).

[104] M. Moskalets and M. Büttiker, Phys. Rev. B **66**, 205320 (2002).

[105] P. Hänggi, *Quantum Transport and Dissipation* (Wiley-VCH, Weinheim, 1998), Chap. 5, pp. 249–286.

[106] U. Peskin and N. Moiseyev, J. Chem. Phys. **99**, 4590 (1993).

[107] M. Holthaus, Z. Phys. B **89**, 251 (1992).

[108] H. Risken, *The Fokker-Planck Equation*, Vol. 18 of *Springer Series in Synergetics*, 2nd ed. (Springer, Berlin, 1989).

[109] T. Holstein, Ann. Phys. (N.Y.) **8**, 325 (1959).

[110] M. Olson, Y. Mao, T. Windus, M. Kemp, M. A. Ratner, N. Leon, and V. Mujica, J. Chem. Phys. **102**, 941 (1998).

[111] Z. G. Yu, D. L. Smith, A. Saxena, and A. R. Bishop, Phys. Rev. B **59**, 16001 (1999).

[112] T. Brandes and B. Kramer, Phys. Rev. Lett. **83**, 3021 (1999).

[113] E. G. Emberly and G. Kirczenow, Phys. Rev. B **61**, 5740 (2000).

[114] M. K. Okuyama and F. G. Shi, Phys. Rev. B **61**, 8224 (2000).

[115] H. Ness, S. A. Shevlin, and A. J. Fisher, Phys. Rev. B **63**, 125422 (2001).

[116] J. Lehmann, G.-L. Ingold, and P. Hänggi, Chem. Phys. **281**, 199 (2002).

[117] E. G. Petrov, V. May, and P. Hänggi, Chem. Phys. **281**, 211 (2002).

[118] D. Segal and A. Nitzan, Chem. Phys. **281**, 235 (2002).

[119] V. May, Phys. Rev. B **66**, 245411 (2002).

[120] P. Talkner, Ann. Phys. (N.Y.) **167**, 390 (1986).

[121] Yu. V. Nazarov, Physica B **189**, 57 (1993).

[122] B. L. Hazelzet, M. R. Wegewijs, T. H. Stoof, and Yu. V. Nazarov, Phys. Rev. B **63**, 165313 (2001).

[123] T. Brandes, Phys. Rev. B **56**, 1213 (1997).

[124] A. Keller, O. Atabek, M. Ratner, and V. Mujica, J. Phys. B **35**, 4981 (2002).

[125] A. Tikhonov, R. D. Coalson, and Y. Dahnovsky, J. Chem. Phys. **116**, 10909 (2002).

[126] J. R. Tucker, IEEE J. Quantum Electron. **QE-15**, 1234 (1979).

[127] J. R. Tucker and M. J. Feldman, Rev. Mod. Phys. **57**, 1055 (1985).

[128] F. Großmann, P. Jung, T. Dittrich, and P. Hänggi, Z. Phys. B **84**, 315 (1991).

[129] C. E. Creffield and G. Platero, Phys. Rev. B **66**, 235303 (2002).

[130] H. Y. Carr and E. M. Purcell, Phys. Rev. **94**, 630 (1954).

[131] U. Haeberlen and J. S. Waugh, Phys. Rev. **175**, 453 (1968).

[132] C. P. Slichter, *Principles of Magnetic Resonance*, Vol. 1 of *Springer Series in Solid State Sciences*, 3 ed. (Springer, Berlin, 1990).

[133] M. A. Ratner, J. Phys. Chem. **94**, 4877 (1990).

[134] P. Reimann and P. Hänggi, Appl. Phys. A **75**, 169 (2002).

[135] R. D. Astumian and P. Hänggi, Physics Today **55**, 33 (2002).

[136] R. P. Feynman, R. B. Leighton, and M. Sands, *The Feynman Lectures on Physics* (Addison Wesley, Reading MA, 1963), Vol. 1, Chap. 46.

[137] I. Goychuk, M. Grifoni, and P. Hänggi, Phys. Rev. Lett. **81**, 649 (1998), erratum: ibid. **81**, 2837 (1998).

[138] I. Goychuk and P. Hänggi, Europhys. Lett. **43**, 503 (1998).

[139] I. Goychuk and P. Hänggi, J. Phys. Chem. B **105**, 6642 (2001).

[140] L. P. Kouwenhoven, A. T. Johnson, N. C. van der Vaart, and C. J. P. M. Harmans, Phys. Rev. Lett. **67**, 1626 (1991).

[141] L. DiCarlo, C. M. Marcus, and J. S. Harris, Jr., Phys. Rev. Lett. **91**, 246804 (2003).

[142] S. Flach, O. Yevtushenko, and Y. Zolotaryuk, Phys. Rev. Lett. **84**, 2358 (2000).

[143] P. Reimann, Phys. Rev. Lett. **86**, 4992 (2001).

[144] J. J. Sakurai, *Modern Quantum Mechanics*, 2nd ed. (Addison-Wesley, Reading, 1995).

[145] A. Aviram and M. A. Ratner, Chem. Phys. Lett. **29**, 277 (1974).

[146] J. Chen, M. A. Reed, A. M. Rawlett, and J. M. Tour, Science **286**, 1550 (1999).

[147] M. Holthaus and D. Hone, Phys. Rev. B **47**, 6499 (1993).

[148] I. M. Gradshteyn and I. S. Ryzhik, *Table of Integrals, Series, and Products*, 5th ed. (Academic Press, San Diego, 1994).

[149] M. Wagner, Phys. Rev. B **49**, 16544 (1994).

[150] M. Wagner, Phys. Rev. A **51**, 798 (1995).

[151] A. Nitzan, M. Galperin, G.-L. Ingold, and H. Grabert, J. Chem. Phys. **117**, 10837 (2002).

[152] S. Pleutin, H. Grabert, G.-L. Ingold, and A. Nitzan, J. Chem. Phys. **118**, 3756 (2003).

[153] G. C. Liang, A. W. Ghosh, M. Paulsson, and S. Datta, Phys. Rev. B **69**, 115302 (2004).

[154] T. Dittrich, B. Oelschlägel, and P. Hänggi, Europhys. Lett. **22**, 5 (1993).

[155] T. Dittrich, F. Grossmann, P. Jung, B. Oelschlägel, and P. Hänggi, Physica A **194**, 173 (1993).

[156] D. E. Makarov and N. Makri, Phys. Rev. E **52**, R2257 (1995).

[157] F. Grossmann, T. Dittrich, P. Jung, and P. Hänggi, J. Stat. Phys. **70**, 229 (1993).

Selected publications

[A1] J. Lehmann, S. Kohler, P. Hänggi, and A. Nitzan,
Molecular wires acting as coherent quantum ratchets,
Phys. Rev. Lett. **88**, 228305 (2002).

[A2] S. Kohler, J. Lehmann, S. Camalet, and P. Hänggi,
Resonant laser excitation of molecular wires,
Israel J. Chem. **42**, 135 (2002).

[A3] J. Lehmann, S. Camalet, S. Kohler, and P. Hänggi,
Laser controlled molecular switches and transistors,
Chem. Phys. Lett. **368**, 282 (2003).

[A4] J. Lehmann, S. Kohler, P. Hänggi, and A. Nitzan,
Rectification of laser-induced electronic transport through molecules,
J. Chem. Phys. **118**, 3283 (2003).

[A5] S. Camalet, J. Lehmann, S. Kohler, and P. Hänggi,
Current noise in ac-driven nanoscale conductors,
Phys. Rev. Lett. **90**, 210602 (2003).

[A6] S. Kohler, S. Camalet, M. Strass, J. Lehmann, G.-L. Ingold, and P. Hänggi,
Charge transport through a molecule driven by a high-frequency field,
Chem. Phys. **296**, 243 (2004).

[A7] K. M. Fonseca-Romero, S. Kohler, and P. Hänggi,
Coherence control for qubits,
Chem. Phys. **296**, 307 (2004).

[A8] S. Kohler, J. Lehmann, M. Strass, and P. Hänggi,
Molecular wires in electromagnetic fields,
Adv. Solid State Phys. **44**, 151 (2004).

[A9] S. Camalet, S. Kohler, and P. Hänggi,
Shot noise control in ac-driven nanoscale conductors,
to appear in Phys. Rev. B; cond-mat/0402182.

[A10] J. Lehmann, S. Kohler, V. May, and P. Hänggi,
Vibrational effects in laser-driven molecular wires,
J. Chem. Phys. **121** (2004), in press; cond-mat/0403614.